

NUCLEON PARTON DISTRIBUTION FUNCTIONS FROM BOOSTED CORRELATORS IN CG

Jinchen He

GHP Meeting

2025/03



UNIVERSITY OF
MARYLAND

Argonne 
NATIONAL LABORATORY

Contents

1

Introduction

- ◆ Parton Physics & PDFs
- ◆ Lattice QCD Calculations of PDFs

2

Methodology

- ◆ LaMET
- ◆ Coulomb Gauge (CG) Method

3

Lattice Calculation with the CG Method

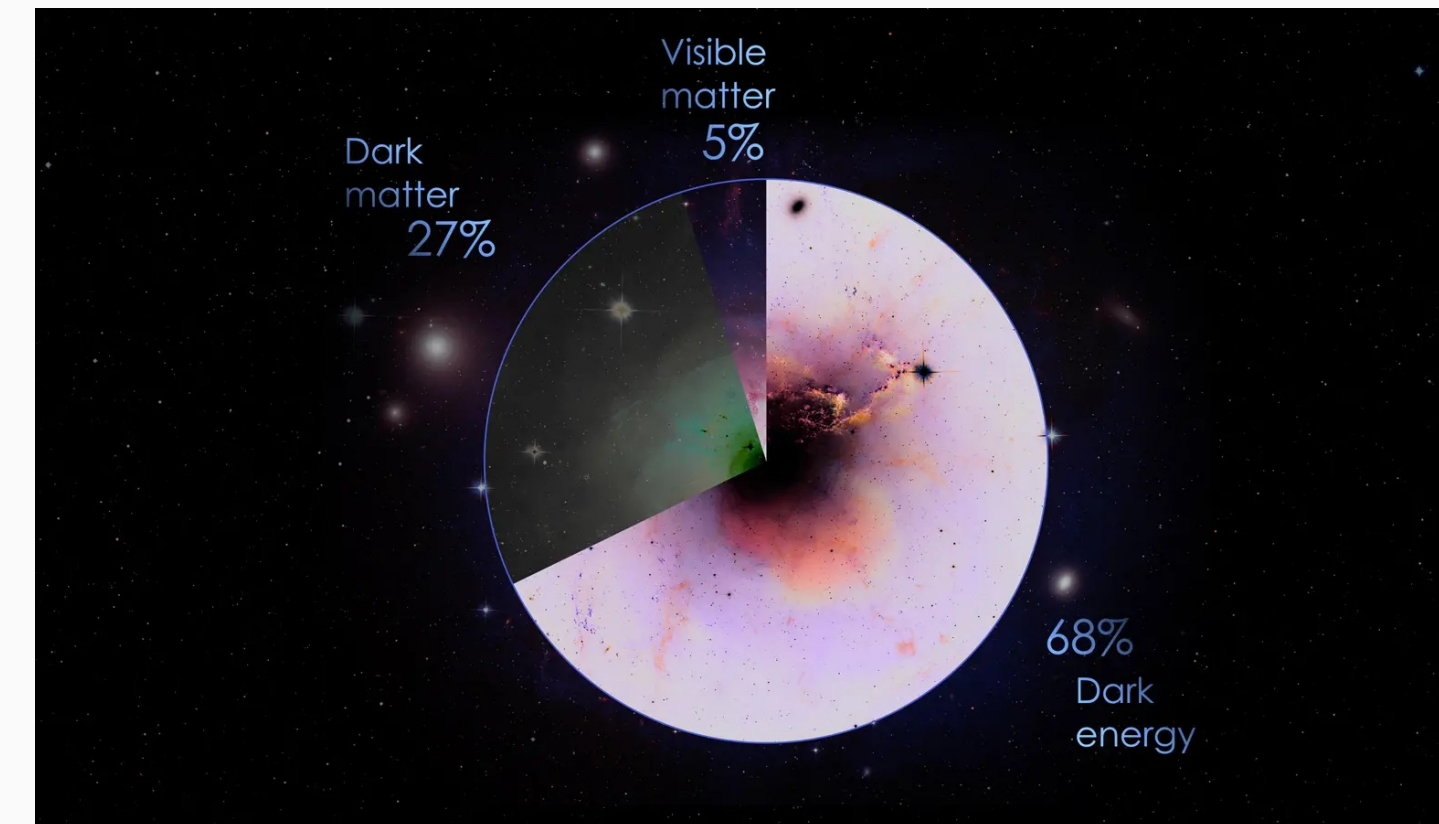
- ◆ Lattice Matrix Elements
- ◆ Renormalization
- ◆ Unpolarized and Helicity Nucleon PDFs

4

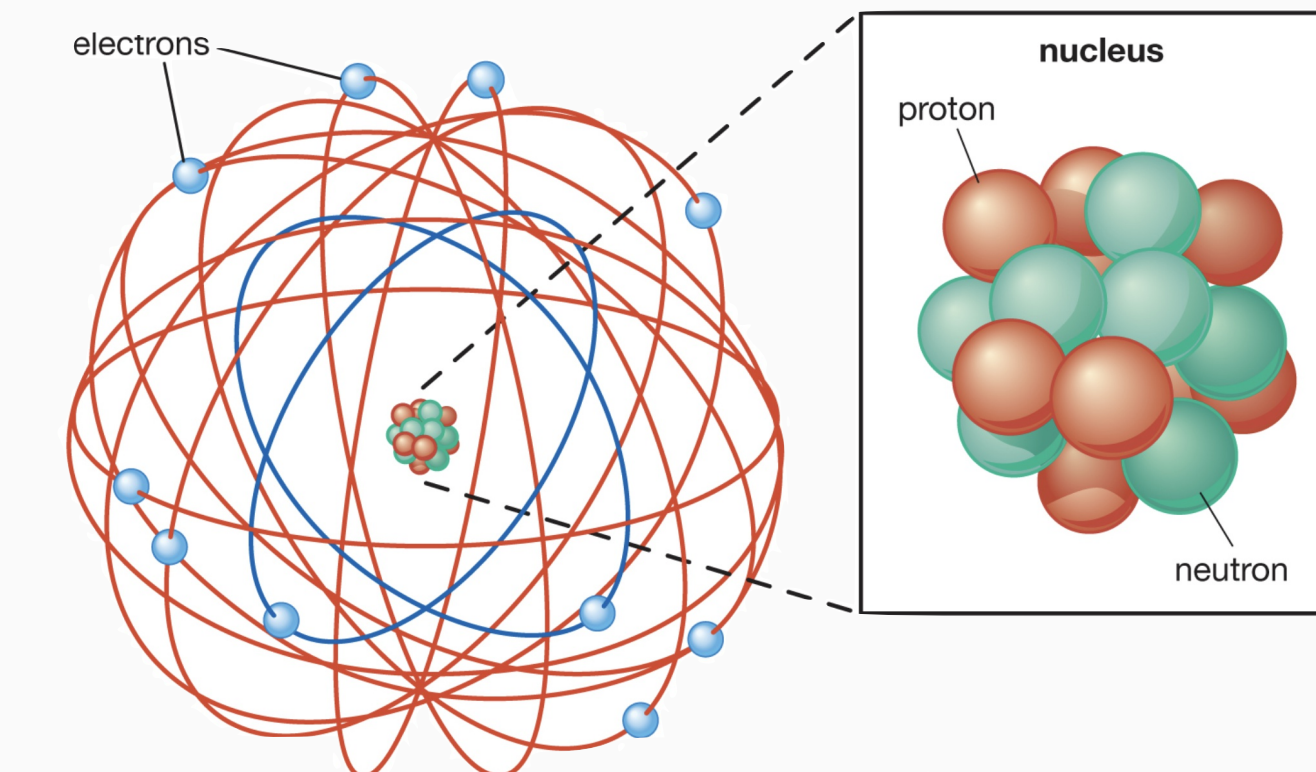
Summary

Visible Universe

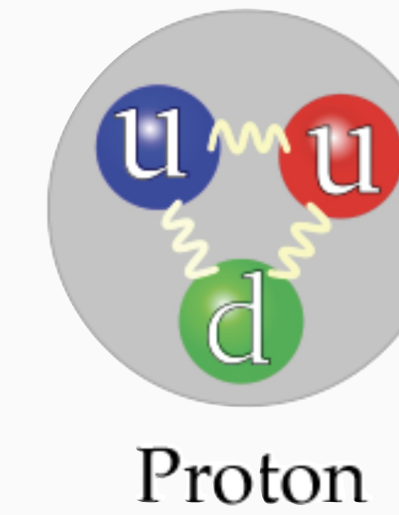
- Only 5% of the universe is visible. *Spergel, David N. "The dark side of cosmology: Dark matter and dark energy." Science 347.6226 (2015): 1100-1102.*
- The visible universe is made up of protons and neutrons, the inner structure of nucleons are sophisticated if we step closer.



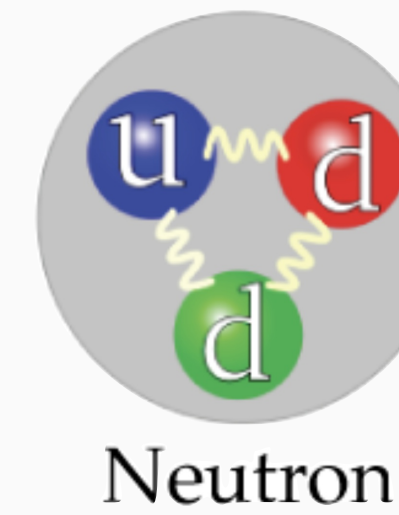
Cr. NASA's Goddard Space Flight Center



© 2012 Encyclopædia Britannica, Inc.



Proton

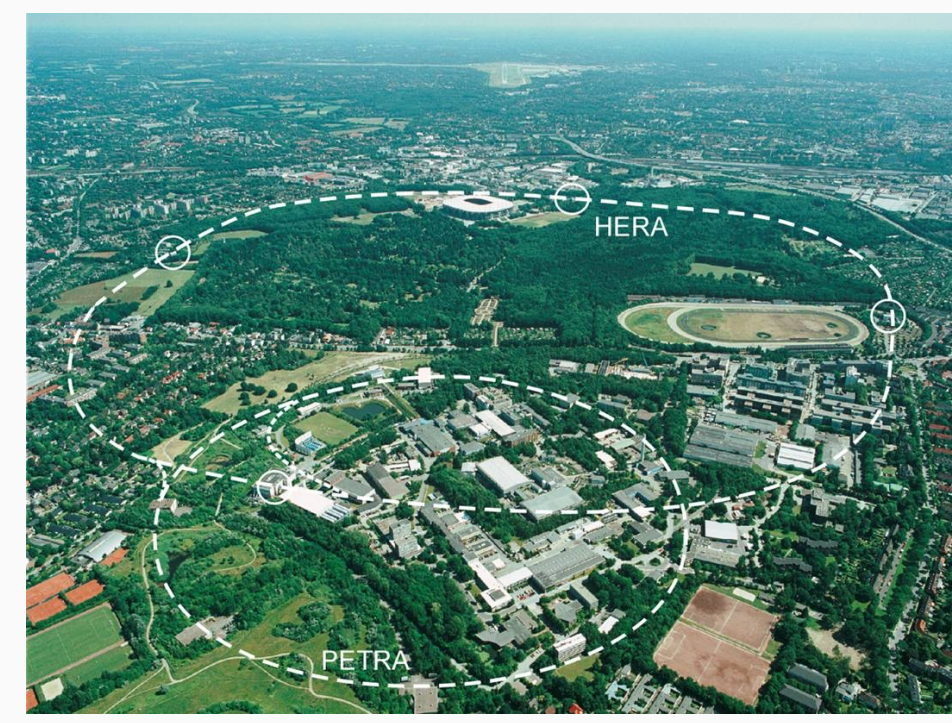
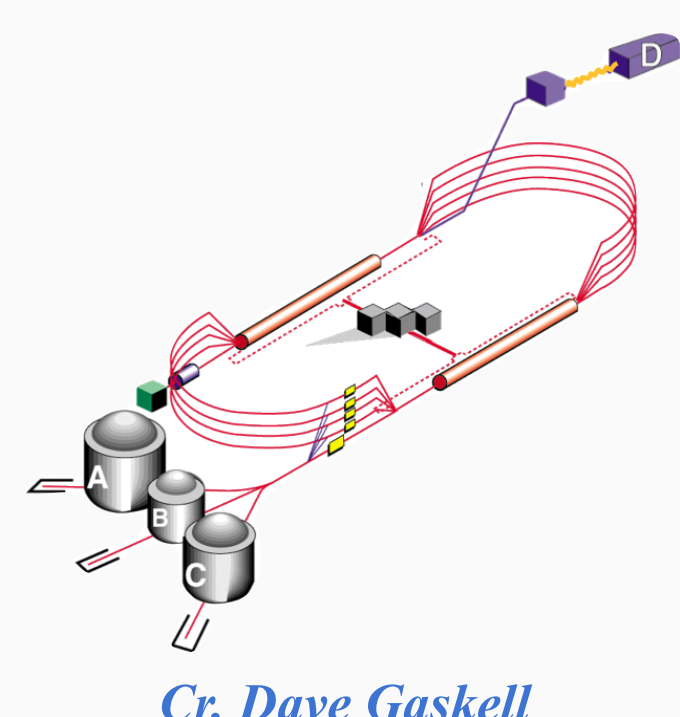


Neutron

- Many experiments have been designed to probe the internal structure of nucleons.

P.S. The list of experiments here is not complete.

CEBAF(JLab)

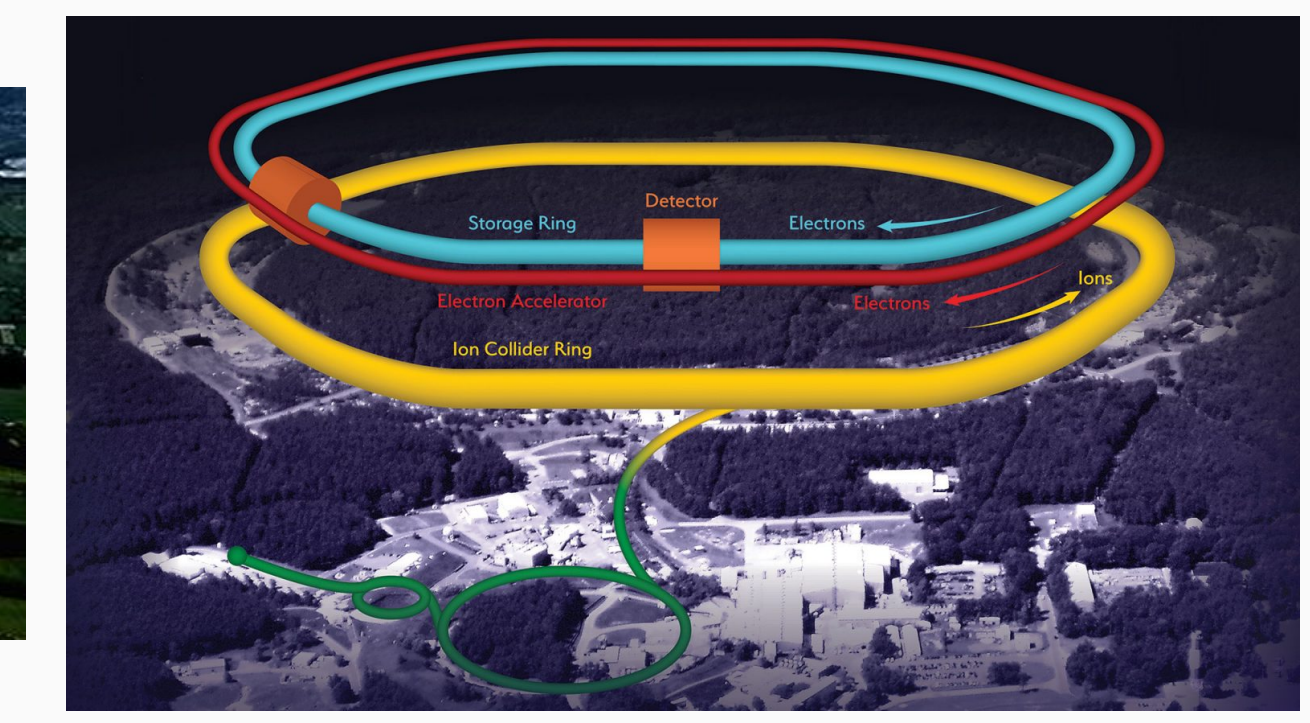


Cr. DESY



Cr. CERN

EIC



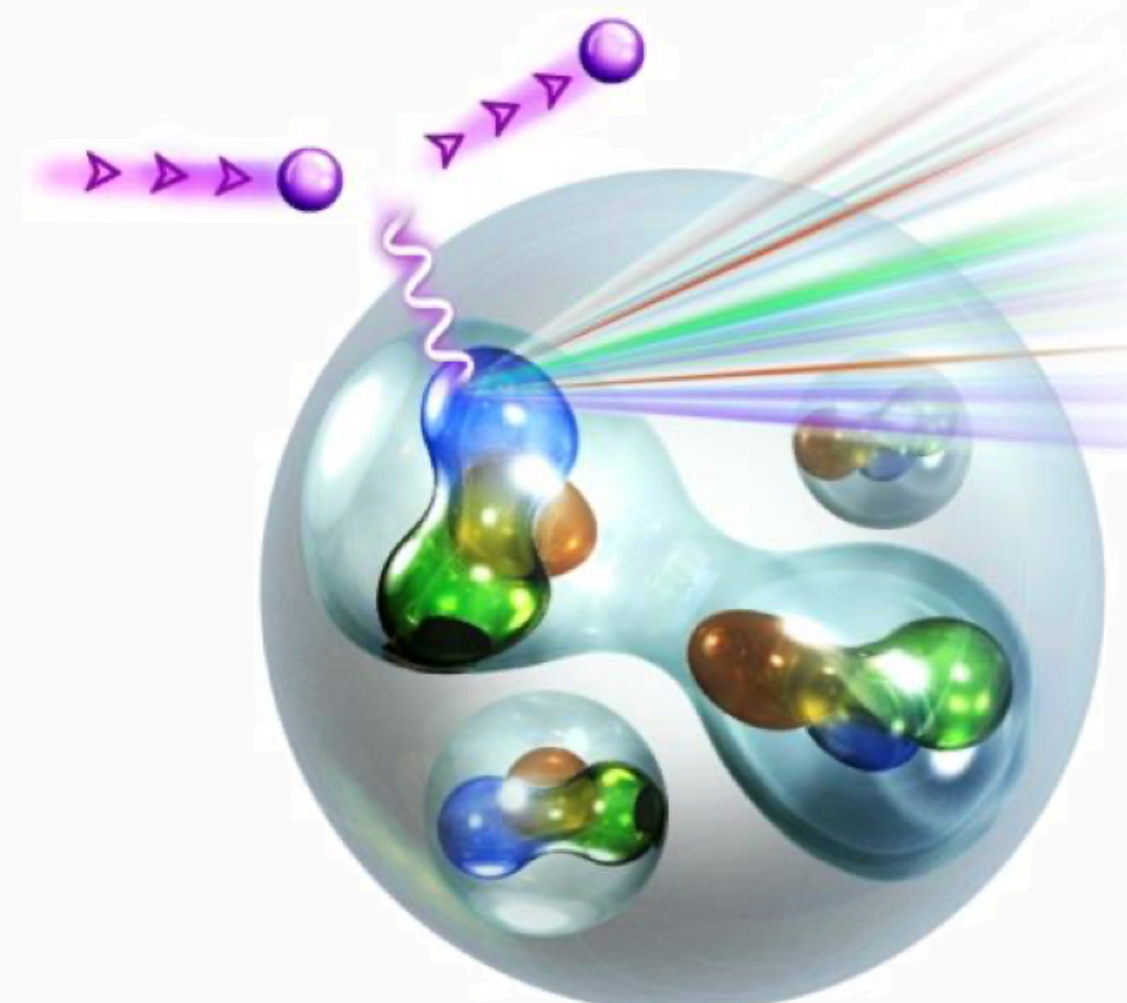
Cr. BNL

Parton Physics

- Our knowledge on proton is still limited:
 - Spin, mass ...
 - How to describe a relativistic moving strong-coupled bound state?
 - The language from Feynman: Parton Model in the infinite momentum frame
R. P. Feynman, Conf. Proc. C 690905 (1969)
 - Quarks and gluons (partons) are ``frozen'' in the transverse plane;
 - During a hard collision, the struck parton appears like a free particle.

R. P. Feynman, Conf. Proc. C 690905 (1969)

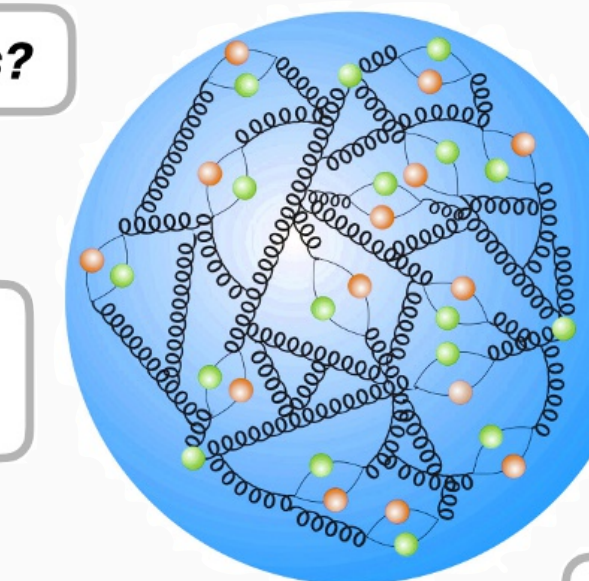
Cr. Juan Rojo



Cr. Dave Gaskell

The many faces of the proton

QCD bound state of quarks and gluons



Origin of mass

Origin of spin?

Gluon-dominated matter?

3D imaging?

Heavy quark content?

Nuclear modifications?

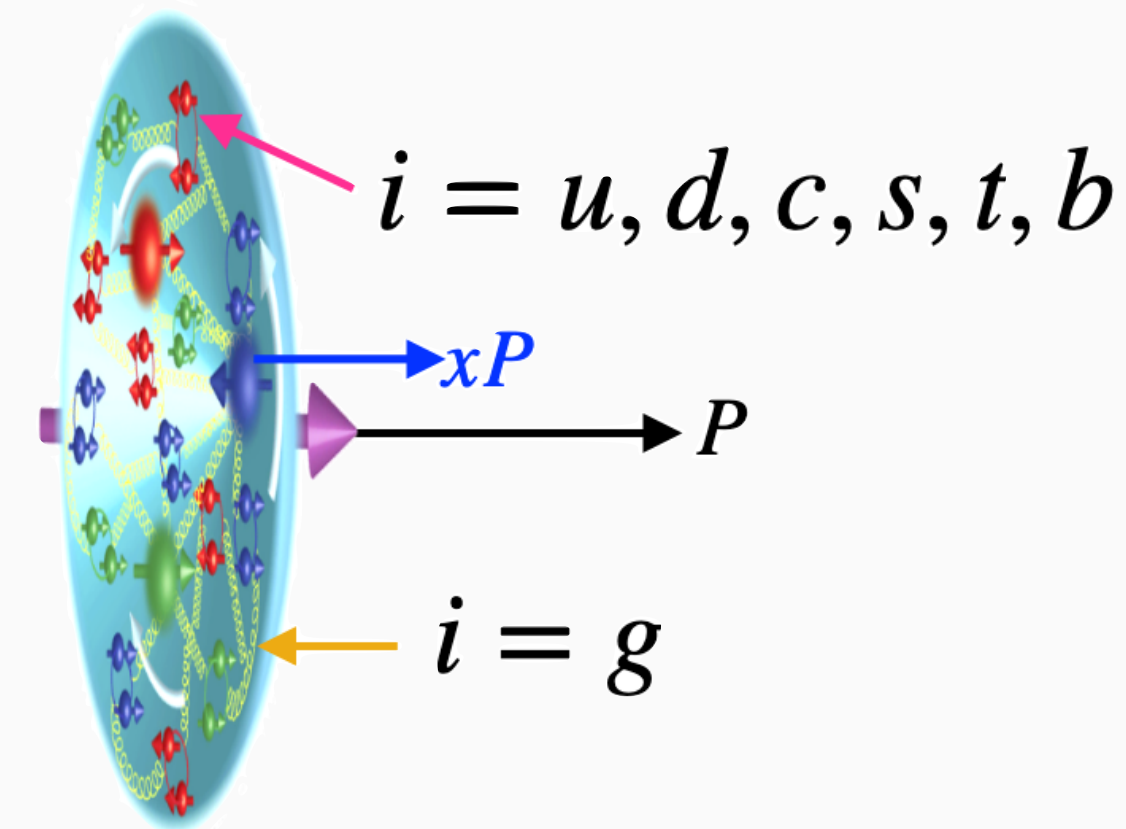
QCD Factorization

The diagram illustrates the factorization of the DIS cross-section. On the left, the DIS cross-section $\sigma_{\text{DIS}} \propto |l|^2$ is shown as the product of two terms: $|l|^2$ (from the virtual photon exchange) and $|q|^2$ (from the quark-gluon vertex). This is followed by a double vertical line and the symbol \approx . To the right of this, the PDF factor $|k|^2 \approx \xi P$ is shown as the product of $|P|^2$ (from the incoming nucleon) and $|\xi P|^2$ (from the gluon exchange). Finally, the perturbative scattering factor $|l'|^2$ is shown as the product of $|l|^2$ (from the virtual photon exchange) and $|\xi P|^2$ (from the gluon exchange), preceded by a crossed circle symbol (\otimes).

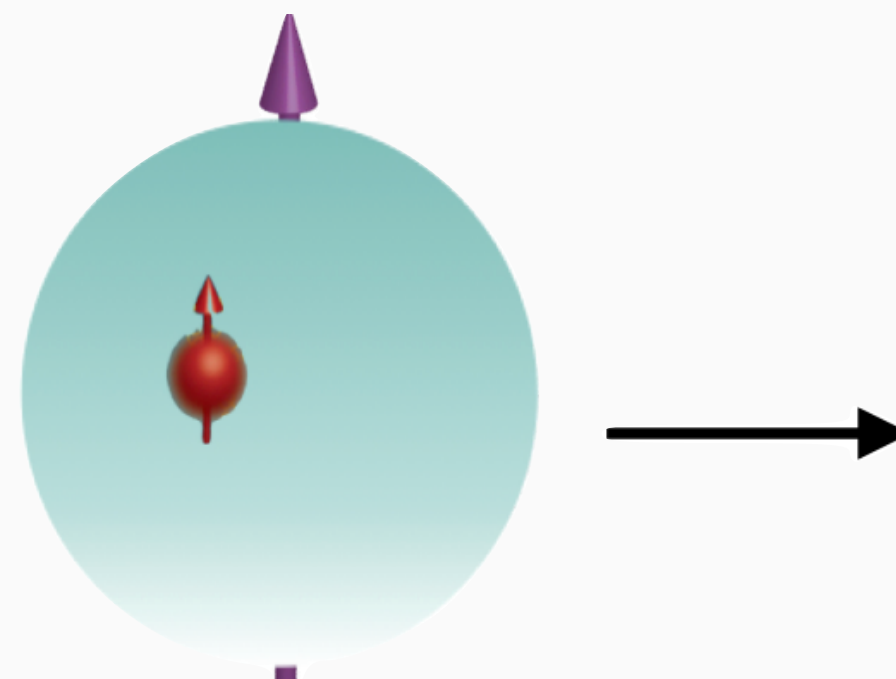
R. Boussarie, et al., “TMD Handbook”, [arXiv:2304.03302 [hep-ph]]

Parton Distribution Functions (PDFs)

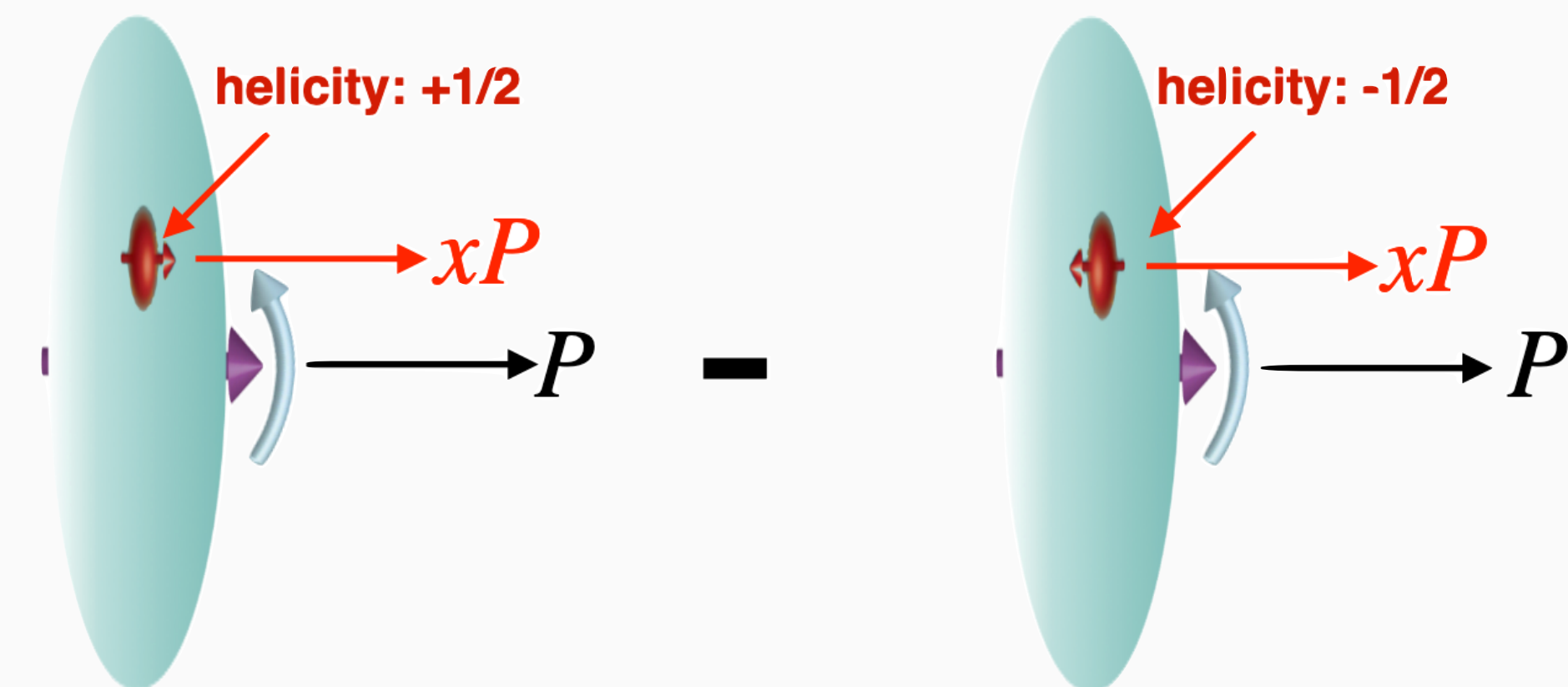
- Unpolarized PDF $f(x, \mu)$: probability distribution



- Transversity PDF $h_1(x, \mu)$: parton contribution to the transverse polarization of hadron

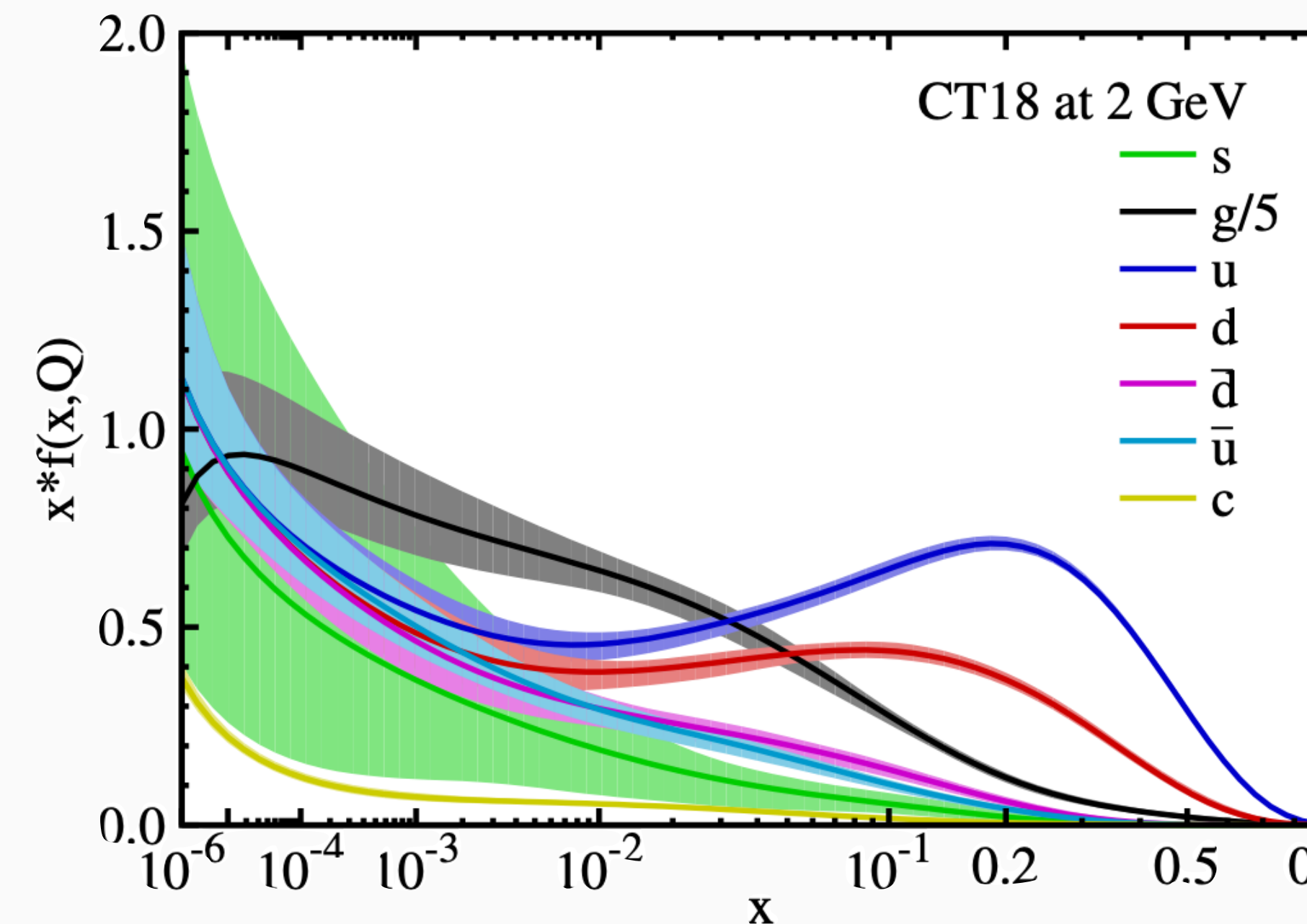


- Helicity PDF $g(x, \mu)$: parton contribution to the hadron spin

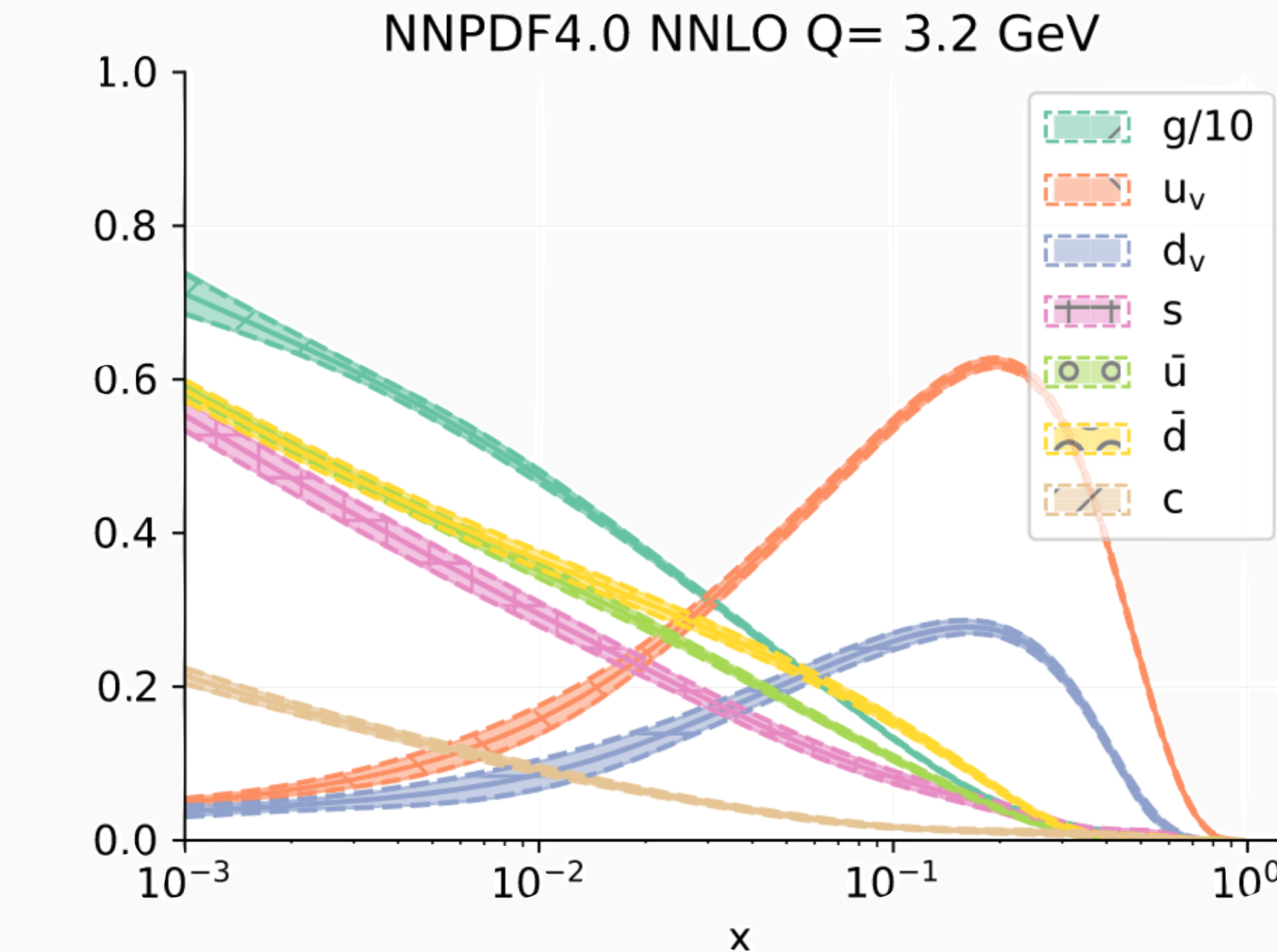


Global Analysis of PDFs

- Since PDFs are universal and useful in scattering processes, many efforts have been spent in extracting PDFs from experimental data.



T. J. Hou, et al., Phys. Rev. D 103 (2021)



R. D. Ball, et al. [NNPDF], Eur. Phys. J. C 82 (2022)

Parameterization form as prior of fit

$$f_i(x, Q_0) = a_0 x^{a_1-1} (1-x)^{a_2} P_i(y; a_3, a_4, \dots)$$

$$x f_k(x, Q_0; \boldsymbol{\theta}) = A_k x^{1-\alpha_k} (1-x)^{\beta_k} \text{NN}_k(x; \boldsymbol{\theta})$$

Lattice QCD Calculation of PDFs

- As a first-principle non-perturbative method, Lattice QCD provides independent predictions of PDFs.
 - Mellin Moments
 - Up to $\langle x^3 \rangle$ [C. Alexandrou, et al., Phys. Rev. D 92 \(2015\); G. S. Bali, et al., Phys. Rev. D 98 \(2018\); ...](#)
 - Smeared operators for higher moments [Z. Davoudi, M. J. Savage, Phys. Rev. D 86 \(2012\); ...](#)
 - Gradient Flow for higher moments [A. Shindler, Phys. Rev. D 110 \(2024\); A. Francis, et al., PoS LATTICE2024, 336 \(2025\); ...](#)
 - Large Momentum Effective Theory (LaMET) (quasi-PDF) [X. Ji, Phys. Rev. Lett. 110 \(2013\); X. Ji, et al., Rev. Mod. Phys. 93 \(2021\); X. Gao, et al., Phys. Rev. Lett. 128 \(2022\); ...](#)
 - Short Distance Expansion
 - Pseudo PDF / Ioffe-time distribution [A. V. Radyushkin, Phys. Rev. D 96 \(2017\); C. Alexandrou, et al., Phys. Rev. D 98 \(2018\); ...](#)
 - Current-current correlator [V. M. Braun, et al., Nucl. Phys. B 685 \(2004\); V. M. Braun, et al., Eur. Phys. J. C 55 \(2008\); R. S. Sufian, et al., Phys. Rev. D 102 \(2020\); ...](#)
 - Operator Product Expansion (OPE)
 - Compton amplitude [A. J. Chambers, et al., Phys. Rev. Lett. 118 \(2017\); M. Gockeler, et al. \[QCDSF\], Phys. Rev. Lett. 92 \(2004\); ...](#)
 - Heavy-quark Operator Product Expansion (HOPE) [W. Detmold, and C. J. David Lin, Phys. Rev. D 73 \(2006\); W. Detmold, et al. \[HOPE\], Phys. Rev. D 105 \(2022\); ...](#)
 - Hadronic Tensor [K. F. Liu, Phys. Rev. D 62 \(2000\); K. F. Liu, and S. J. Dong, Phys. Rev. Lett. 72 \(1994\); ...](#)

Large-Momentum Effective Theory(LaMET)

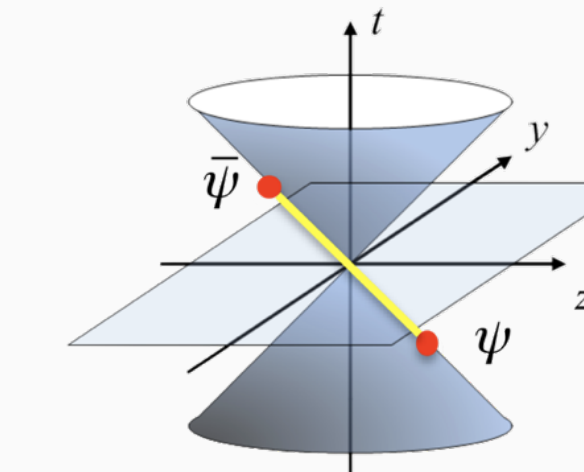
- PDF is defined from a light-cone correlator in a hadron, which is Lorentz invariant.

$$f_\Gamma(x, \mu) = \int_{-\infty}^{\infty} \frac{d\lambda}{2\pi} e^{-i\lambda x} \frac{1}{2P^+} \left\langle P \left| \bar{\psi}(\xi^-) W(\xi^-, 0) \Gamma \psi(0) \right| P \right\rangle \leftrightarrow \left\langle |\vec{P}| = \infty \left| O(t=0) \right| |\vec{P}| = \infty \right\rangle$$

Parton model

- Define a quasi distribution with large-momentum states and time-independent operators.

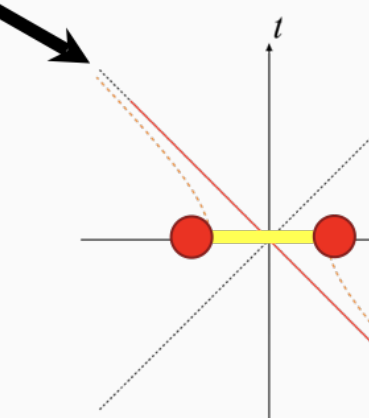
$$\tilde{f}_\Gamma^0(y, P^z, \mu) = P^z \int \frac{dz}{2\pi} e^{iz(yP^z)} \frac{1}{2P^t} \langle P | \bar{\psi}_0(z) W(z, 0) \Gamma \psi_0(0) | P \rangle$$



*X. Ji, Phys.Rev.Lett. 110 (2013)
X. Ji, et al., Rev.Mod.Phys. 93 (2021)
X. Ji, Nucl. Phys. B 1007 (2024)*

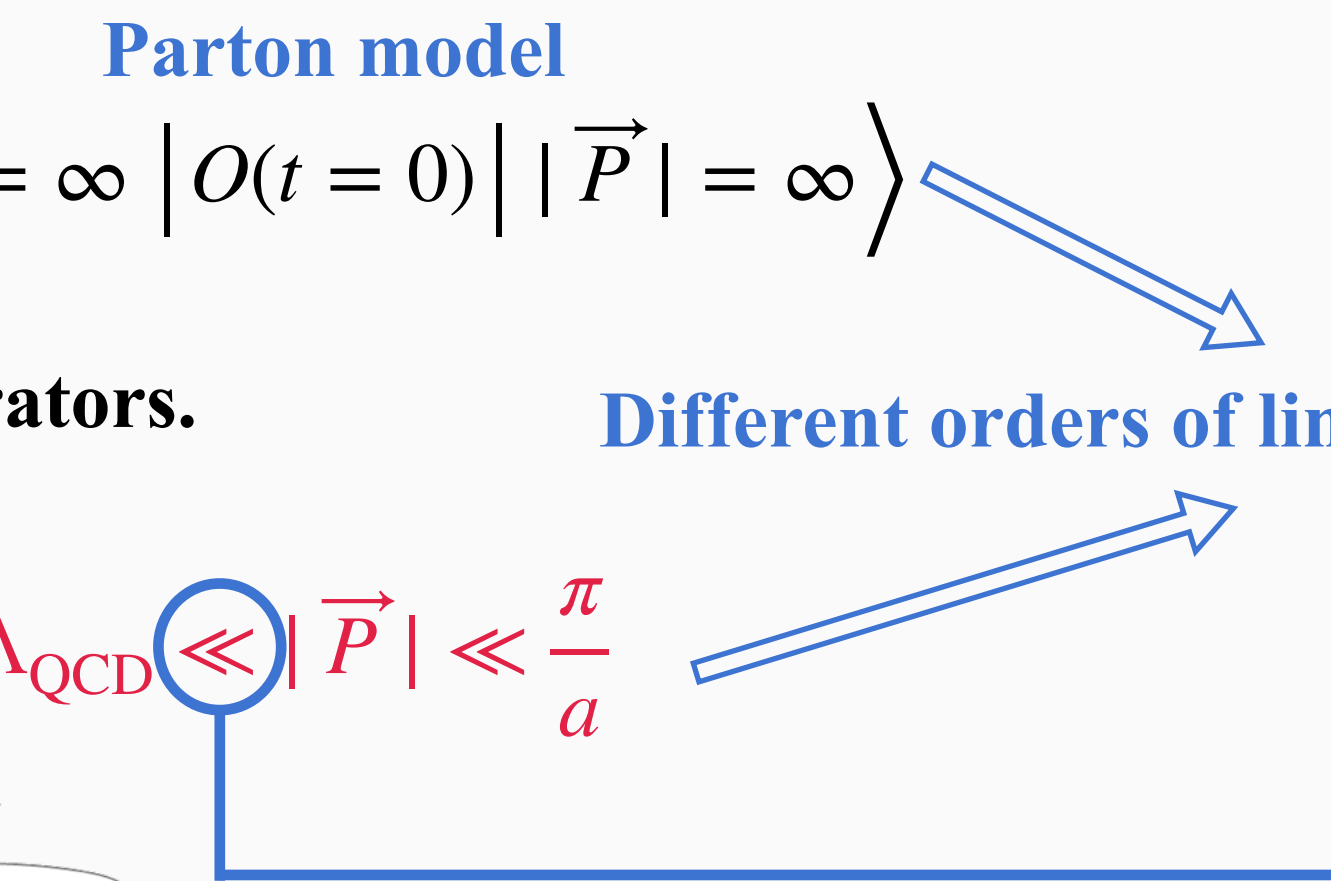
Light-cone distribution:

Cannot be directly calculated on the lattice



Quasi distribution:

Directly calculable on the lattice



- LaMET enables us to obtain the precision-controlled x-distribution of PDFs in $x \in [x_{\min}, x_{\max}]$.

Pert. matching kernel

$$f(x, \mu) = C \left(\frac{y}{x}, \frac{P^z}{\mu} \right) \otimes \tilde{f} \left(y, \frac{P^z}{\mu} \right) + O \left(\frac{\Lambda_{\text{QCD}}^2}{(xP^z)^2}, \frac{\Lambda_{\text{QCD}}^2}{((1-x)P^z)^2} \right)$$

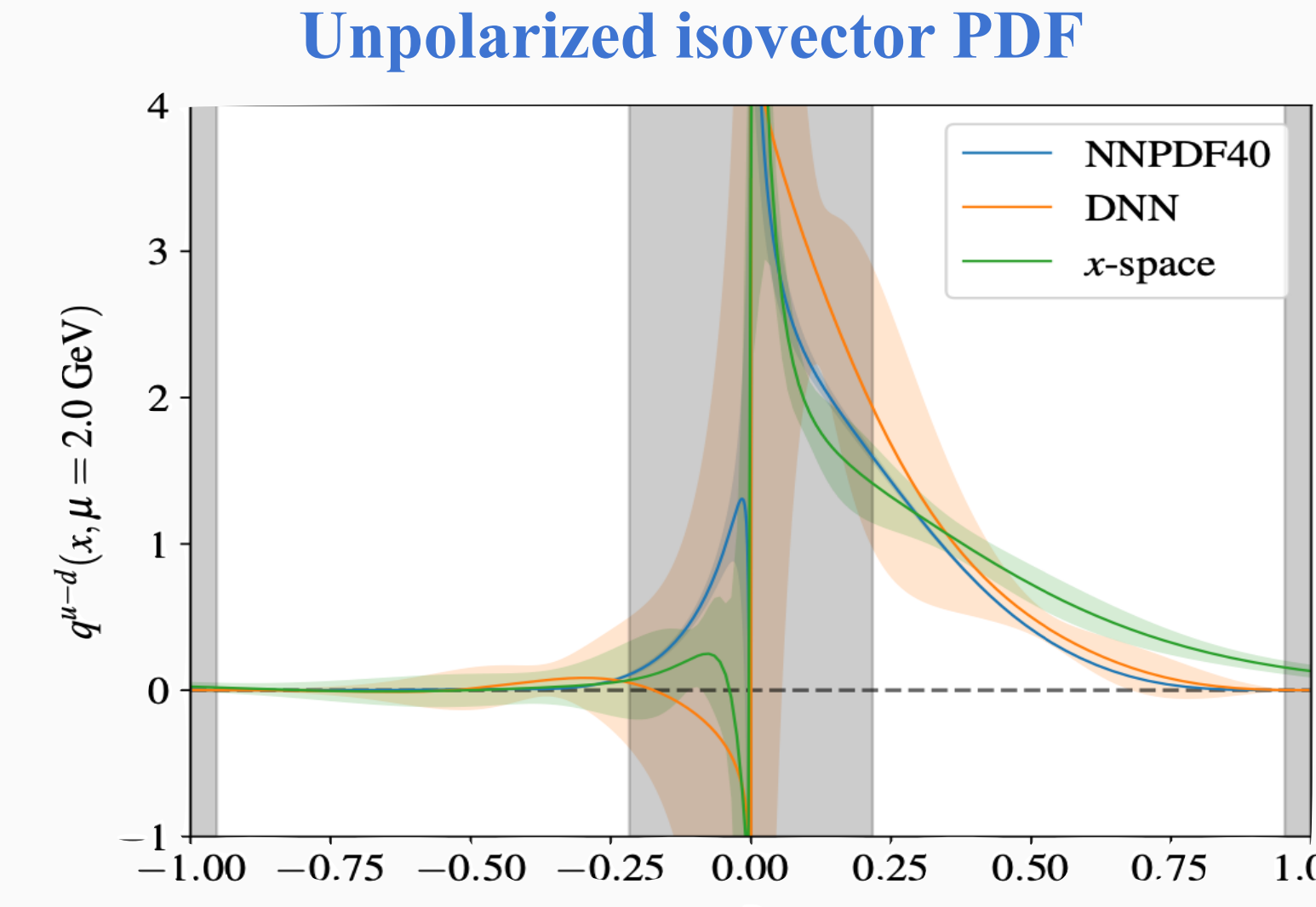
Power corrections

Nucleon PDFs from LaMET

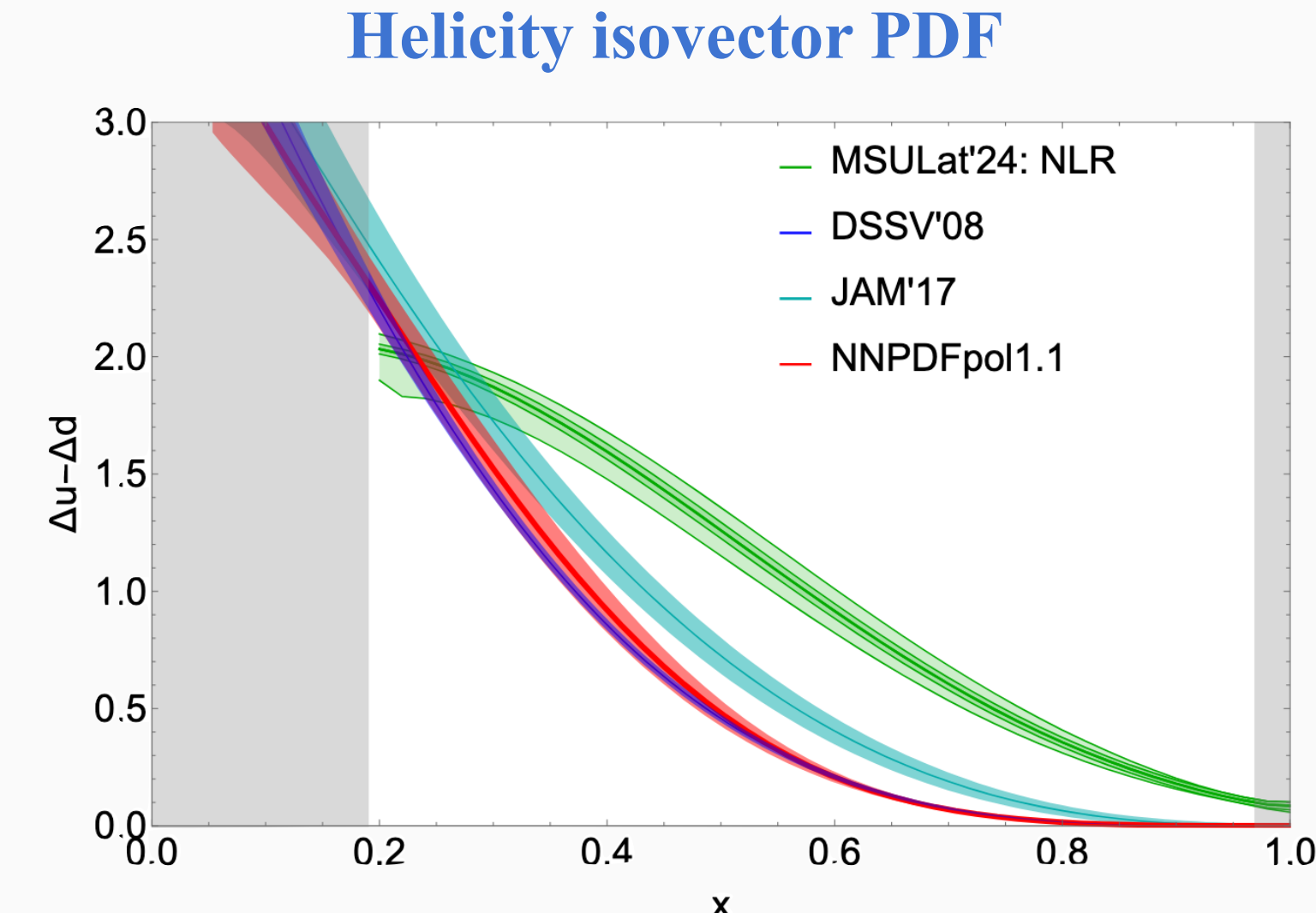
- In recent years, a lot of improvements of renormalization and matching has been developed in LaMET;

[Y. Su, et al., Nucl. Phys. B 991 \(2023\);](#)
[R. Zhang, et al., Phys. Lett. B 844 \(2023\);](#)
[X. Ji, et al., 2410.12910 \[hep-ph\]](#)

- ◆ $a = 0.076 \text{ fm}$
- ◆ $P_{\max}^z = 1.53 \text{ GeV}$
- ◆ Physical m_π^{val}



[X. Gao, et al., Phys. Rev. D 107 \(2023\)](#)



[J. Holligan and H. W. Lin, Phys. Lett. B 854 \(2024\)](#)

- Existing calculations of the nucleon PDFs still deviate from the global analyses, which is possibly due to the systematics from:
 - Hadron momentum is not large enough;
 - Excited-state contamination;
 - Other lattice systematics, like discretization effects, non-physical pion mass, finite volume effects ...

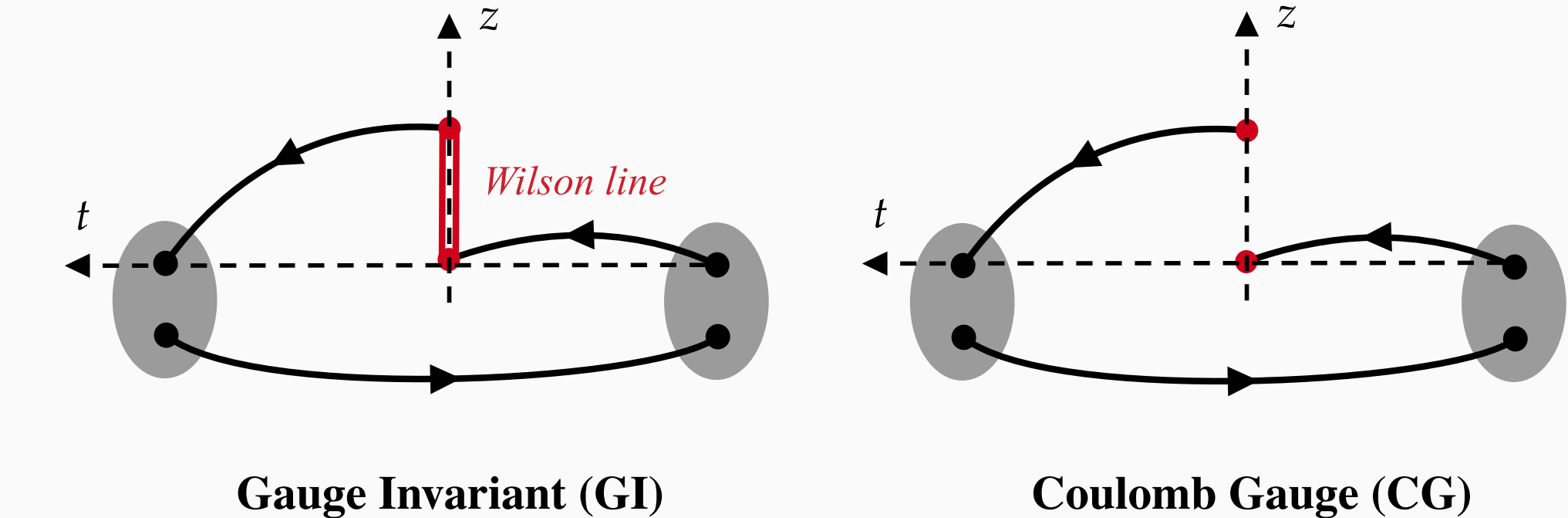
Coulomb Gauge Method

- Define a quasi distribution in CG without Wilson line:

$$\tilde{f}_{\text{CG}}^0(y, P^z, \mu) = P^z \int \frac{dz}{2\pi} e^{iz(yP^z)} \frac{1}{2P^t} \langle P | \bar{\psi}_0(z) \Gamma \psi_0(0) |_{\vec{\nabla} \cdot \vec{A}=0} | P \rangle$$

X. Gao, W. Y. Liu and Y. Zhao, PRD 109 (2024)

Y. Zhao, PRL 133 (2024)

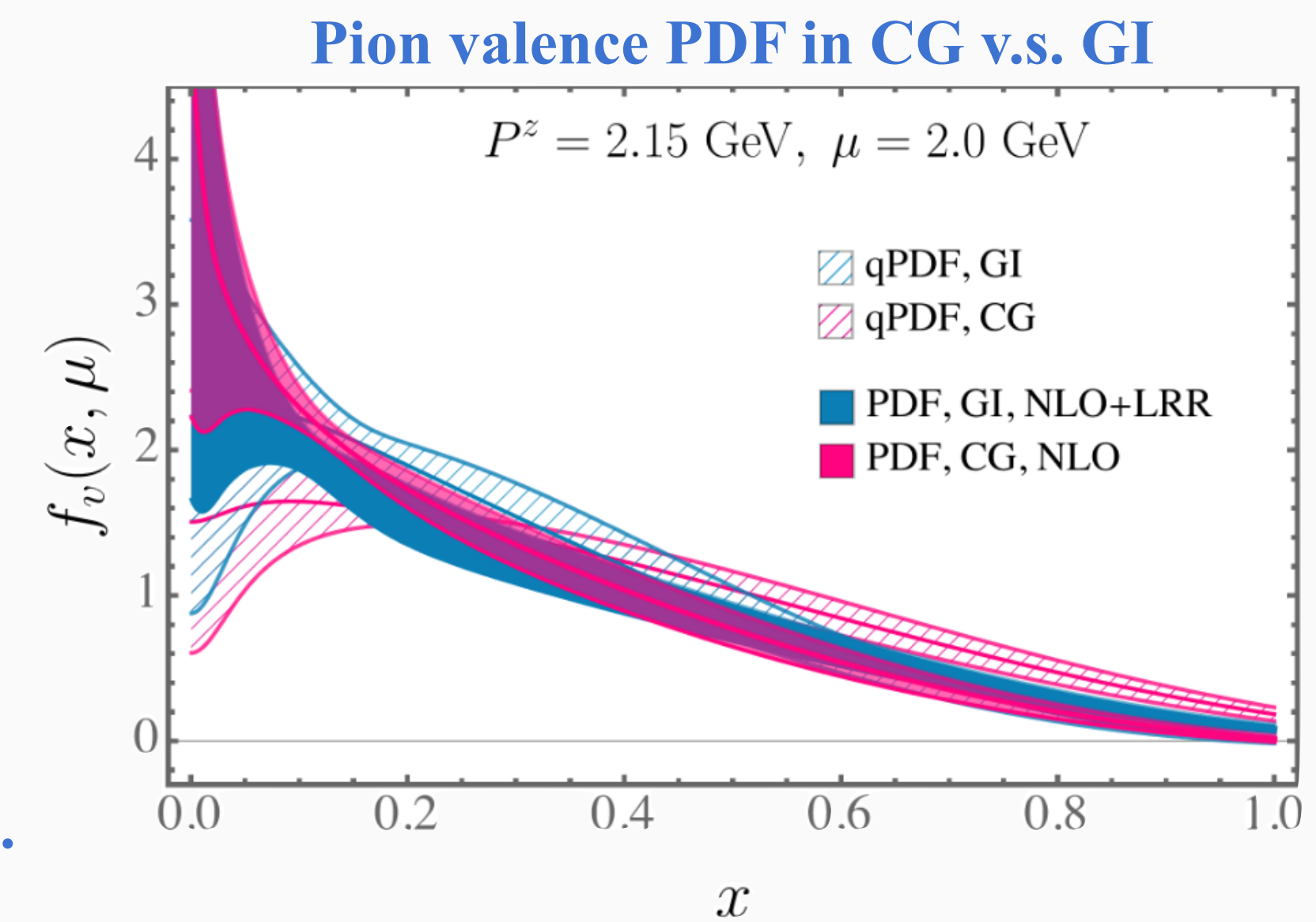


- Why choose CG?

X. Ji, Y. S. Liu, Y. Liu, J. H. Zhang and Y. Zhao, RMP 93 (2021)

- $\vec{\nabla} \cdot \vec{A} = 0$ becomes $A^+ = 0$ in the infinite boost, so the quasi distribution in CG belongs to the universality class in LaMET;
- No linear divergence / linear renormalon;
- Simplified renormalization $\bar{\psi}_0(z) \Gamma \psi_0(0) = Z_\psi(a) [\bar{\psi}(z) \Gamma \psi(0)]$;
- Larger off-axis momenta (3D rotational symmetry).

The results in CG and GI are consistent with the same lattice setup.

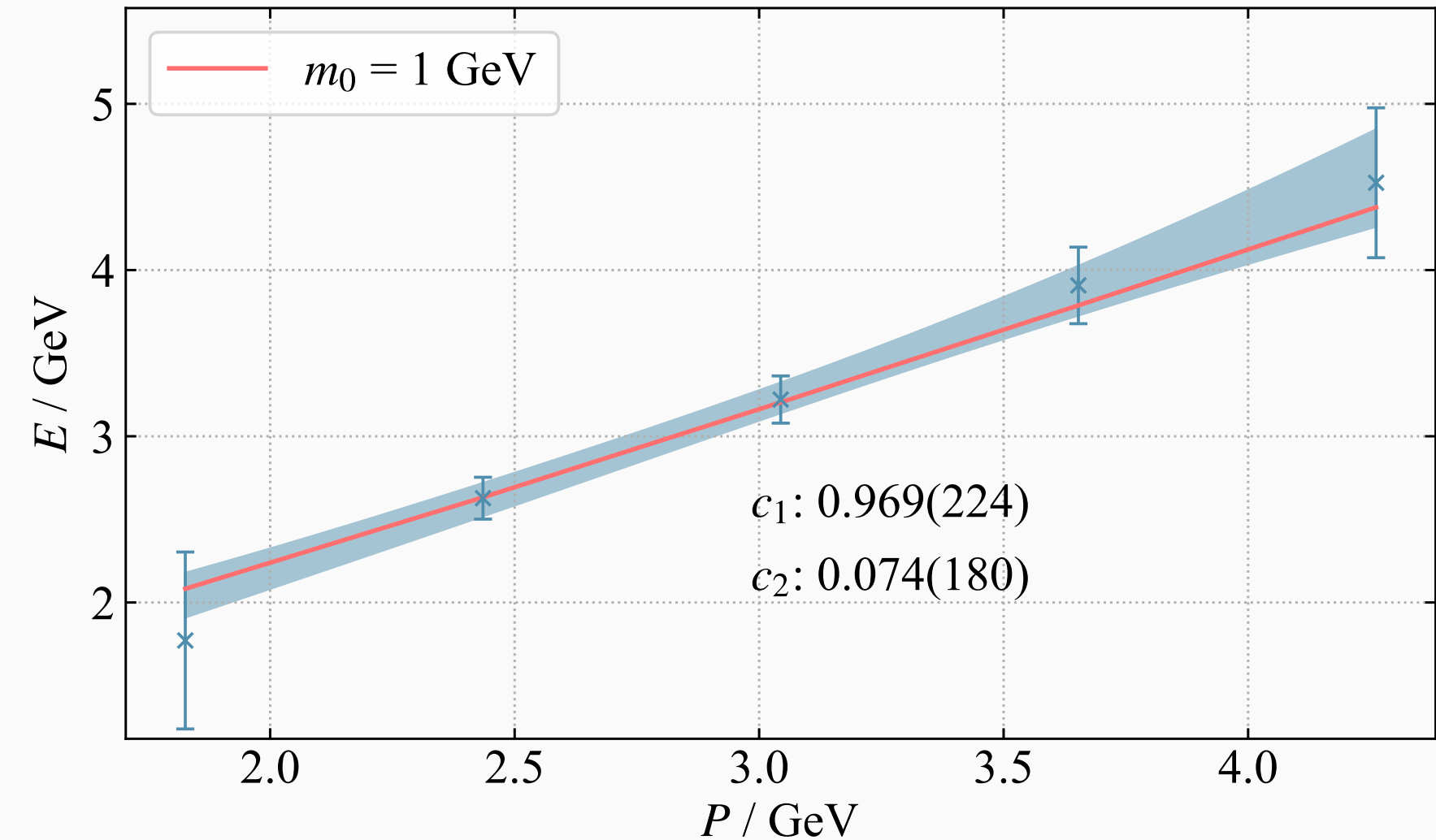


X. Gao, W. Y. Liu and Y. Zhao, PRD 109 (2024)

Lattice Setup for Nucleon Calculation

- **2+1 flavor HISQ ensemble by HotQCD with volume $L_s \times L_t = 48^3 \times 64$;**
- **Lattice spacing is $a = 0.06$ fm;**
- **Pion mass of sea quark: $m_\pi^{\text{sea}} = 160$ MeV;**
- **Pion mass of valence quark: $m_\pi^{\text{val}} = 300$ MeV;**
- **Off-axis ($\vec{n} = (1,1,0)$) hadron momenta: 2.43 GeV and 3.04 GeV;**
- **Statistics for each lattice correlator: 553 (configs) $\times 256$ (inversions) $\times 2$ ($\pm z$ directions) = 283,136;**
- **Gauge fixing criterion: variation of functional satisfies $\delta F/F < 10^{-8}$.**

Dispersion relation: $E^2 = m_0^2 + c_1 P^2 + c_2 a^2 P^4$



Ground State Fit

- Ratio of three-point and two-point correlators

$$R(t_{\text{sep}}, \tau) = \frac{C_{3\text{pt}}(t_{\text{sep}}, \tau)}{C_{2\text{pt}}(t_{\text{sep}})} = \frac{\sum_{n,m} z_n O_{nm} z_m^\dagger \cdot e^{-E_n(t_{\text{sep}} - \tau)} e^{-E_m \tau}}{\sum_n z_n z_n^\dagger \cdot (e^{-E_n t_{\text{sep}}} + e^{-E_n (L_t - t_{\text{sep}})})} \xrightarrow[t_{\text{sep}}, \tau, (L_t - t_{\text{sep}}) \rightarrow \infty]{} O_{00}$$

- Feynman-Hellmann (FH) inspired Method [C. Bouchard, et al., Phys. Rev. D 96 \(2017\)](#)

Cancellation of excited-state contamination.

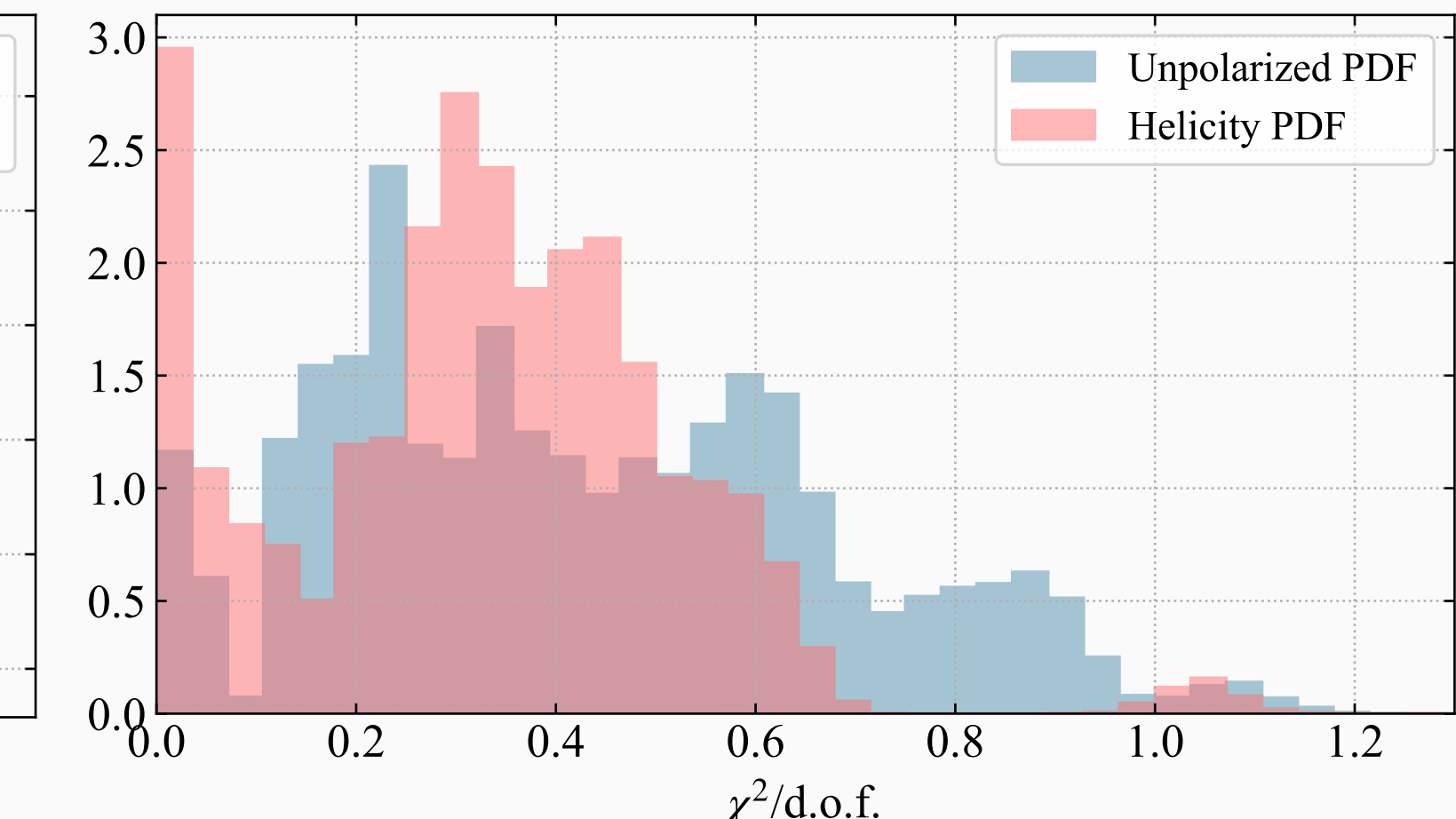
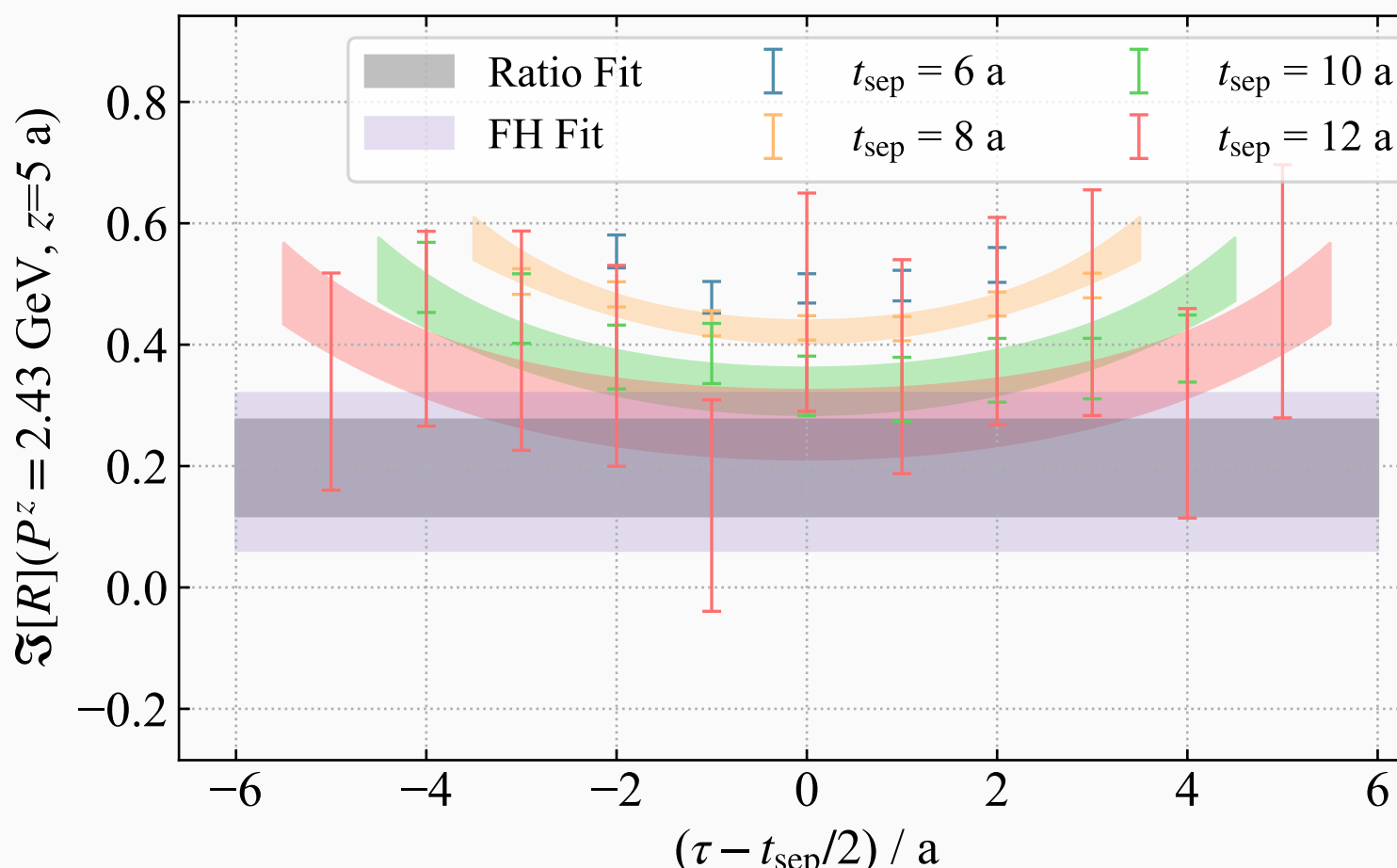
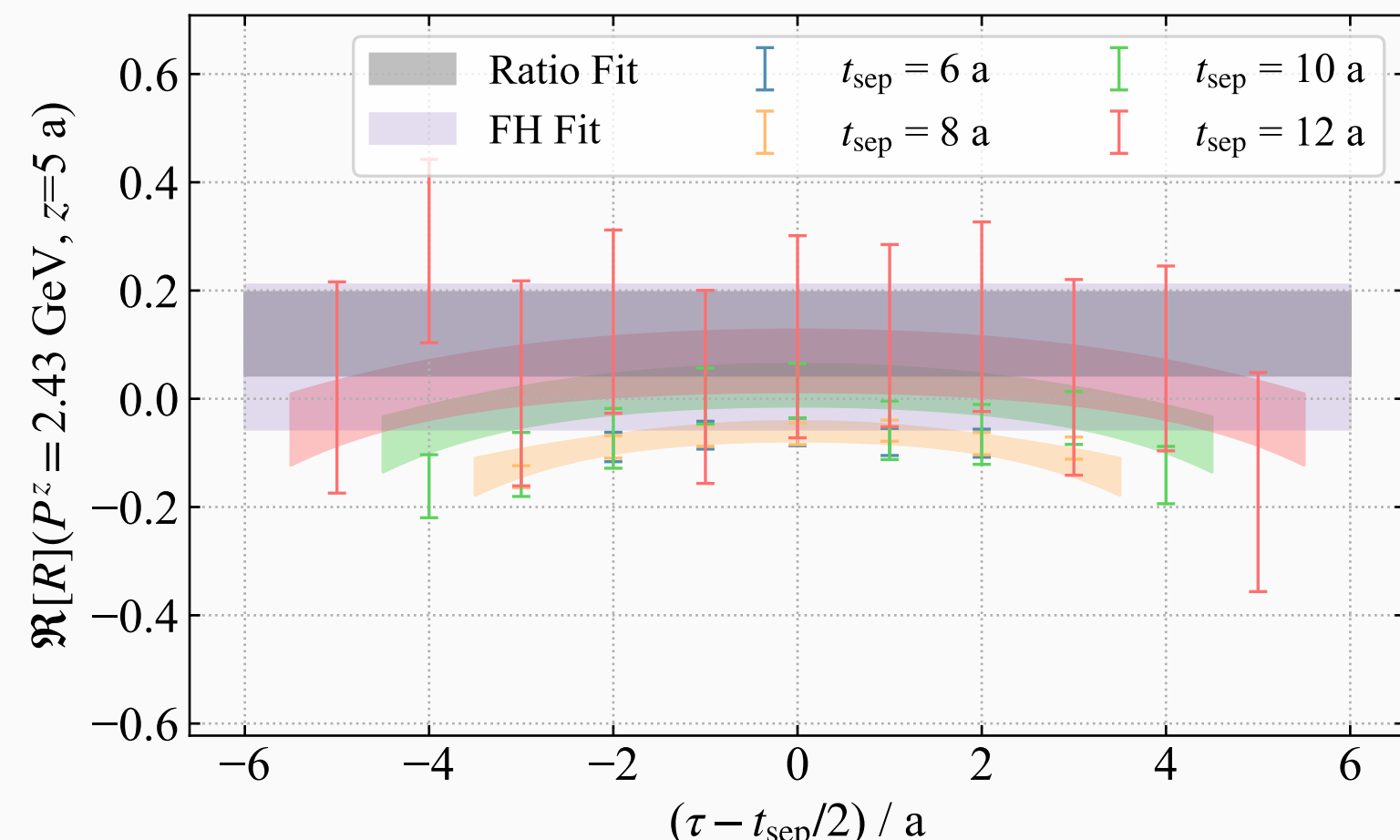
[J. C. He, et al., Phys. Rev. C 105 \(2022\)](#)

$$\text{FH}(t_{\text{sep}}, \tau_{\text{cut}}, dt) \equiv \frac{\sum_{t=\tau_{\text{cut}}}^{t=t_{\text{sep}}+dt-\tau_{\text{cut}}} R(t_{\text{sep}} + dt, t) - \sum_{t=\tau_{\text{cut}}}^{t=t_{\text{sep}}-\tau_{\text{cut}}} R(t_{\text{sep}}, t)}{dt} \xrightarrow[t_{\text{sep}}, \tau, (L_t - t_{\text{sep}}) \rightarrow \infty]{} O_{00}$$

$\chi^2/\text{d.o.f.} < 1.2$ of FH Fit

The ratio fit and FH fit are consistent.

Keep generating more t_{sep} ...



Non-perturbative Renormalization

- Because of the absence of Wilson line, the CG correlation is free from linear divergence, the renormalized operator can be defined as $\bar{\psi}_0(z)\Gamma\psi_0(0) = Z_\psi(a)[\bar{\psi}(z)\Gamma\psi(0)]$;

X. Ji, et al., Nucl. Phys. B 964 (2021)

- Thus, we adopt the hybrid scheme as below, which does not introduce IR effects in the non-perturbative region:

$$\tilde{h}_\Gamma(z, P^z, z_s) = N \frac{\tilde{h}_\Gamma^0(z, P^z, a)}{\tilde{h}_\Gamma^0(z, 0, a)} \theta(z_s - |z|) + N \frac{\tilde{h}_\Gamma^0(z, P^z, a)}{\tilde{h}_\Gamma^0(z_s, 0, a)} \theta(|z| - z_s),$$

where $N = \tilde{h}_\Gamma^0(0, 0, a)/\tilde{h}_\Gamma^0(0, P^z, a)$ and $a \ll z_s \ll 1/\Lambda_{\text{QCD}}$

Note that $\tilde{h}_\Gamma^0(z, 0, a)$ has real part only, which is used to renormalize both the real and imaginary parts of $\tilde{h}_\Gamma^0(z, P^z, a)$.

- The scheme dependence will be cancelled by the hybrid-scheme matching kernel that relates the quasi-PDF to the PDF.

Fourier Transform

- Due to the statistical uncertainty, the quasi-PDF in the large $\lambda = zP^z$ has a finite error bar, which will introduce unphysical fluctuations after Fourier transform;

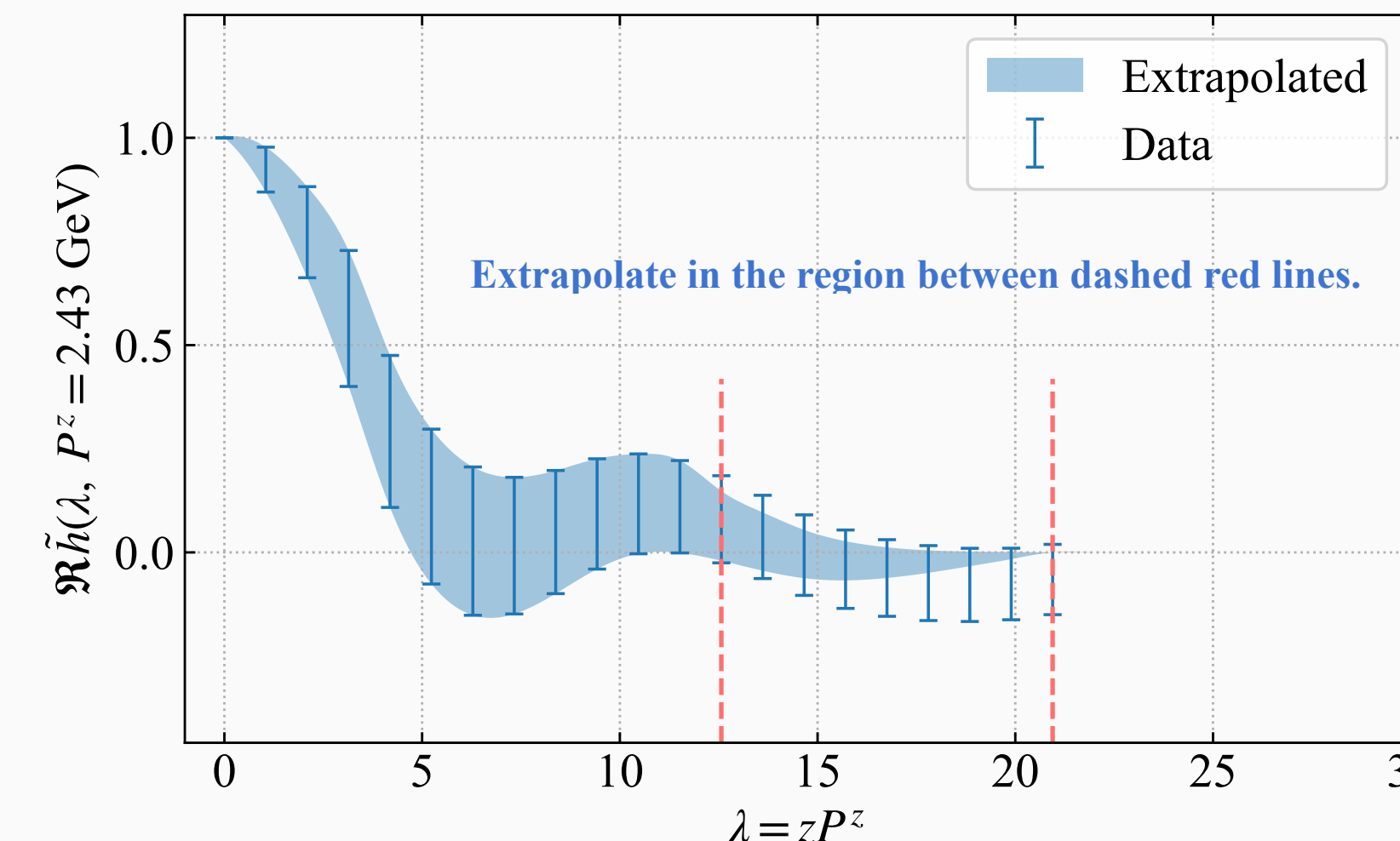
X. Gao, et al., Phys. Rev. Lett. 128 (2022)

- Because of the finite correlation length, the quasi-PDF in coordinate space should decay exponentially in the large z region ($z \sim 1$ fm);
- Since quasi-PDF (in moderate x) is insensitive to the extrapolation strategies, the non-fit extrapolation is adopted here:

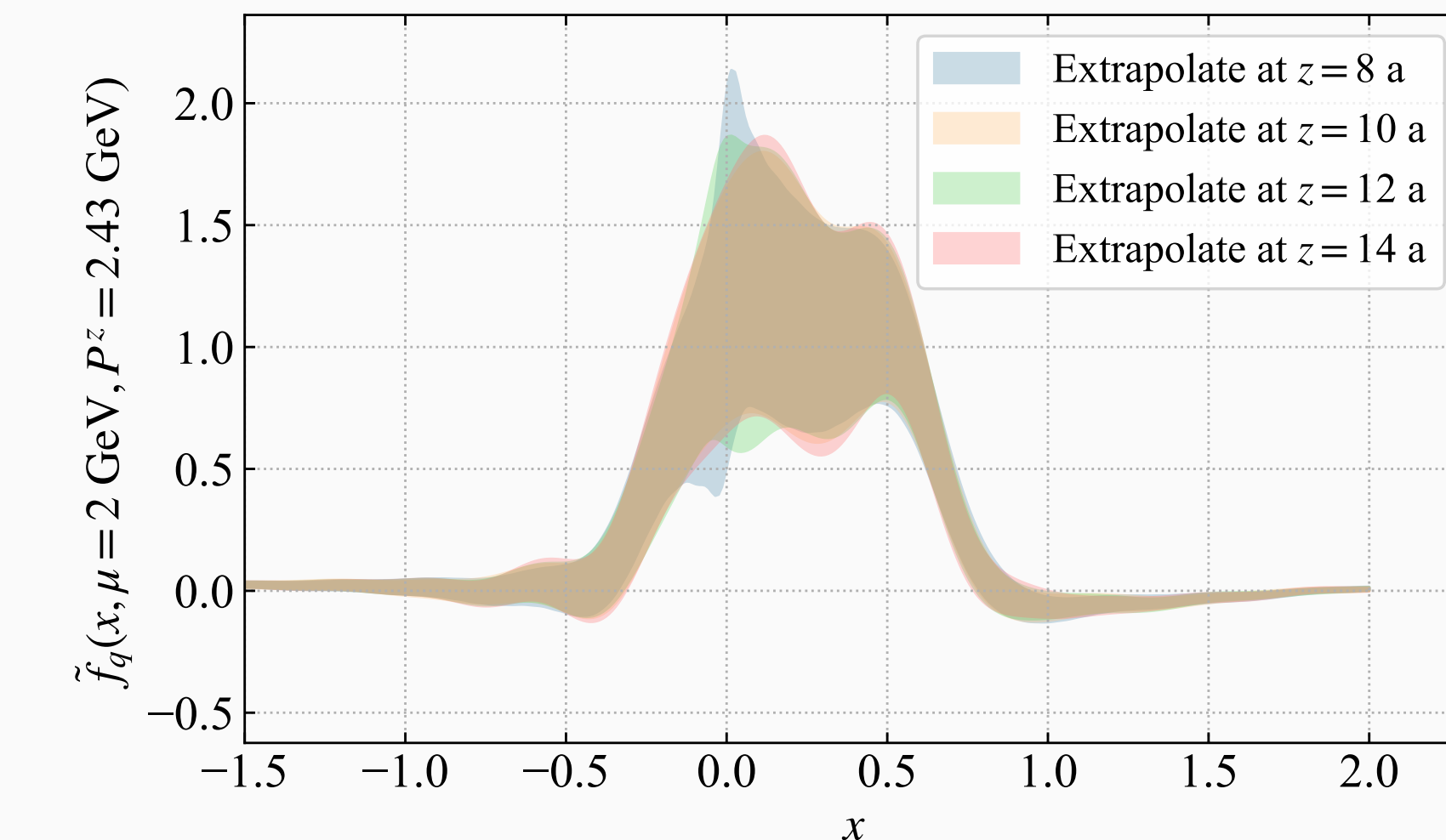
$\tilde{h}^{\text{ext}} = w \cdot \tilde{h} + (1 - w) \cdot 0$, where the weight $w(z)$ linearly decays from 1 to 0 within two red dashed lines below.

- The CG matrix elements decay to zero while the error bars remain almost constant, making the FT easy to be under control.

Unpolarized quasi-PDF in the coordinate space



Comparison of different extrapolation points



Matching to PDFs

- The matching formula for the hybrid-scheme quasi-PDFs

$$f(x, \mu) = \mathcal{C} \left(\frac{x}{y}, \frac{P^z}{\mu}, z_s \right) \otimes \tilde{f} \left(y, \frac{P^z}{\mu}, z_s \right) + O \left(\frac{\Lambda_{\text{QCD}}^2}{(x P^z)^2}, \frac{\Lambda_{\text{QCD}}^2}{((1-x) P^z)^2} \right)$$

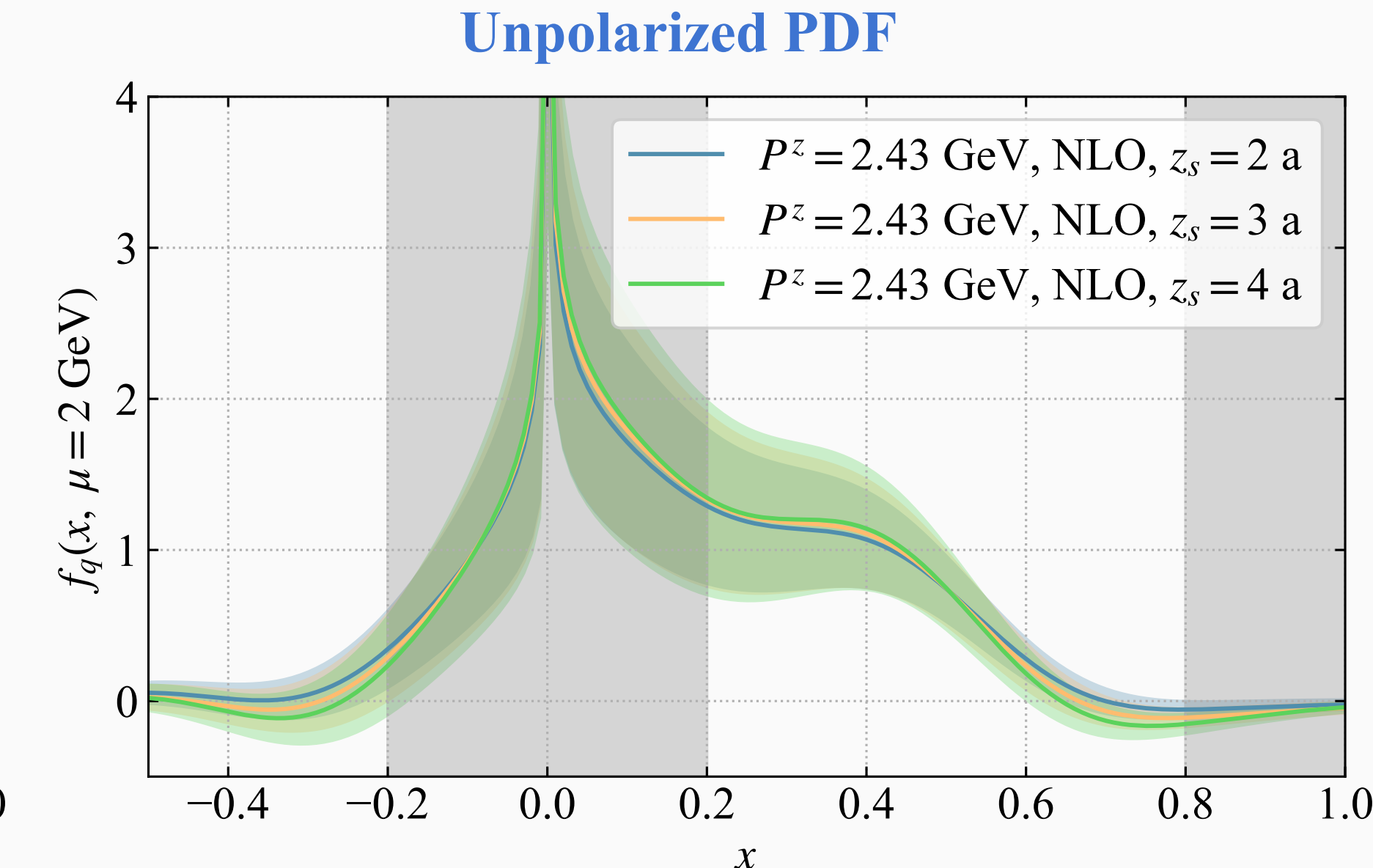
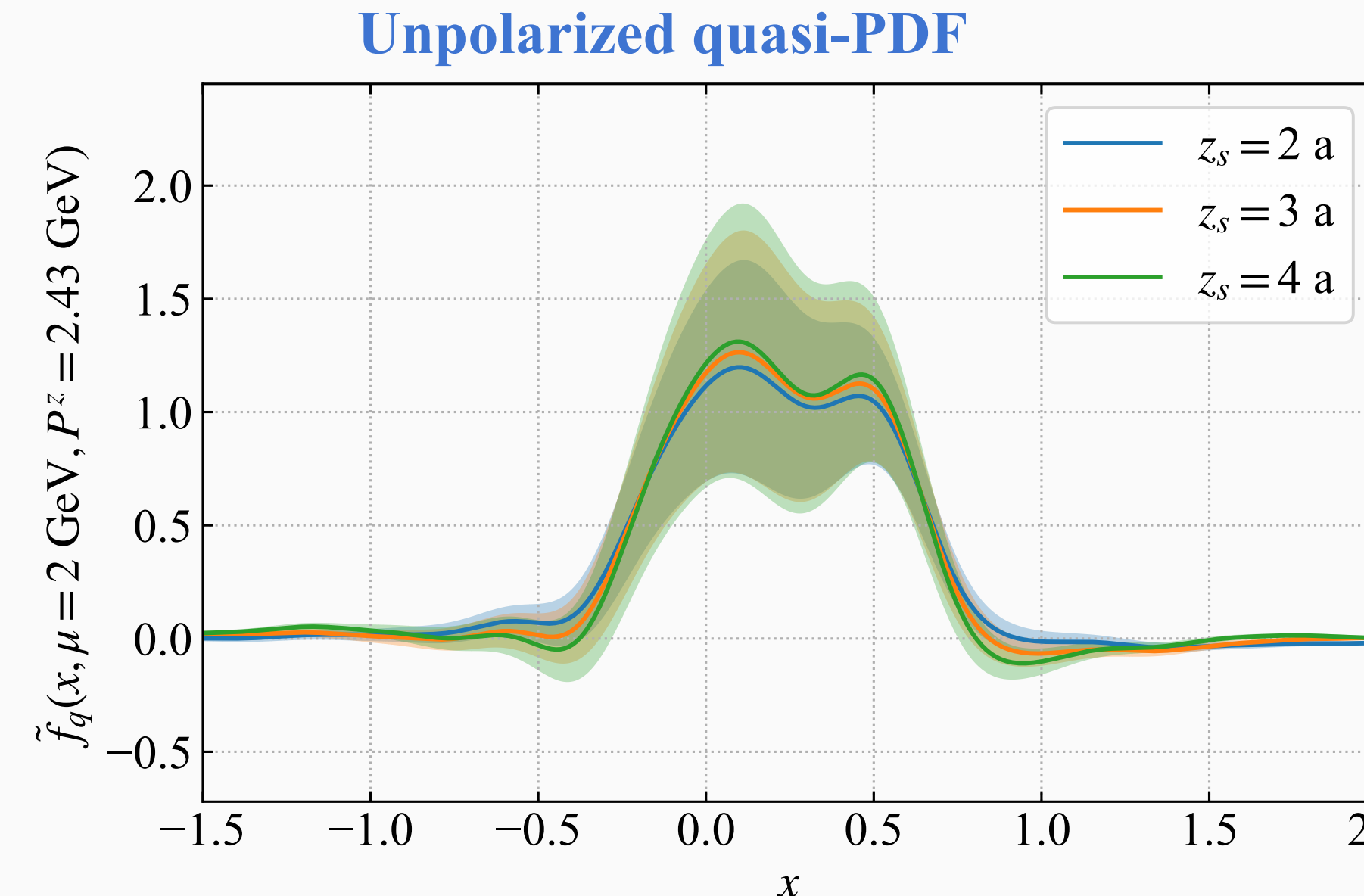
- The matching kernel is calculated using both

- the fixed-order NLO perturbation theory ($\mu = 2$ GeV)

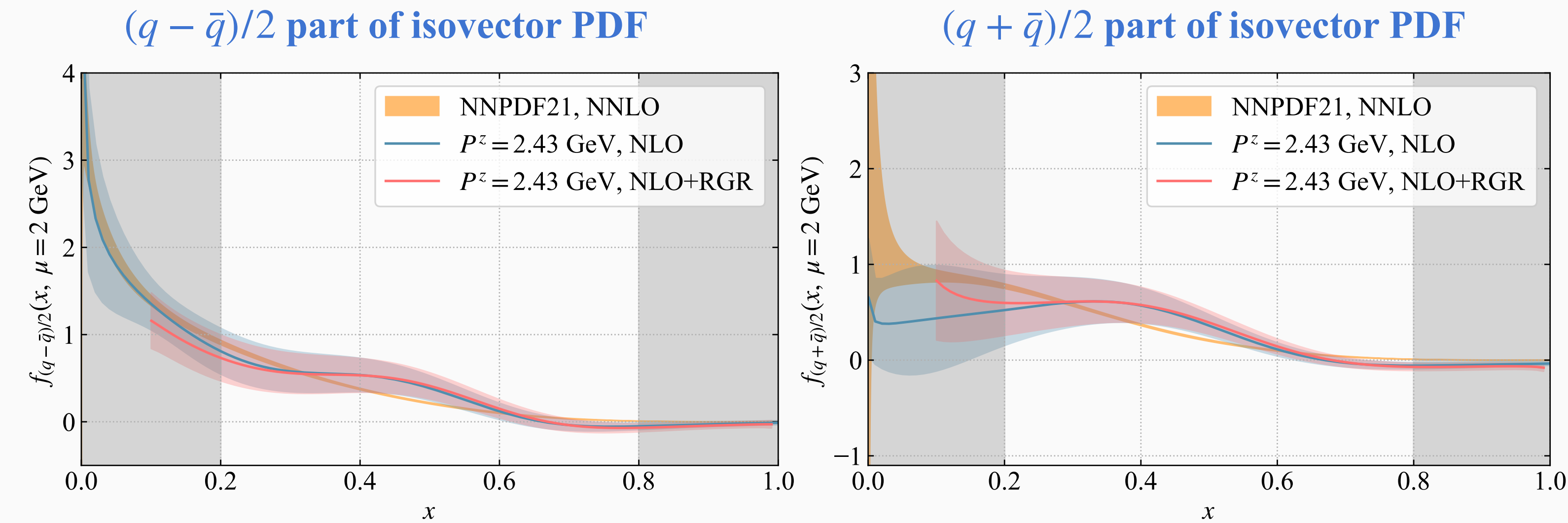
[Y. Su, et al., Nucl. Phys. B 991 \(2023\);](#)

- renormalization group resummed (RGR) NLO perturbation theory (evolve from $\mu \sim 2xP^z$ to $\mu = 2$ GeV)

- The scheme dependence on z_s is cancelled by the matching.



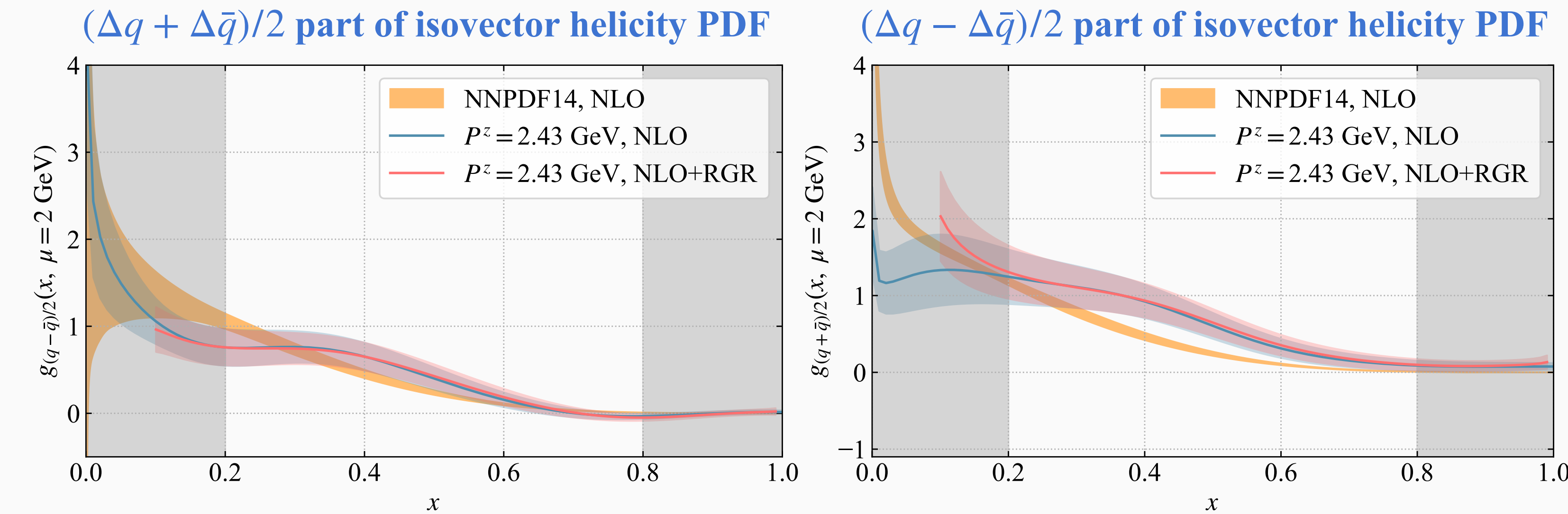
Unpolarized Quark Isovector PDF of Proton



Lattice: [X. Gao, JH, et al. In preparation](#)
NNPDF21: [R. D. Ball, et al. \[NNPDF\], Eur. Phys. J. C 82 \(2022\)](#)

- The **fixed-order** and **RGR** matchings show an aligned behavior at **moderate x** , where LaMET can make reliable prediction;
- Comparing with the NNPDF results, CG method gives a **consistent prediction** on the **valence part** of both the unpolarized and the helicity PDFs, which provides encouraging evidence for the **efficacy of the CG method**;
- The **small deviation of the valence part** might be caused by the **excited-state contamination** and other lattice systematics;
- The deviation of $(q + \bar{q})/2$ from the NNPDF results may be caused by systematics from **excited-state contaminations** and **renormalization of the imaginary part** of quasi PDF matrix elements, which exist in GI method as well;
- This work also serves as an examination of **universality** in LaMET.

Helicity Quark Isovector PDF of Proton



Lattice: [X. Gao, JH, et al. In preparation](#)

NNPDF14: [E. R. Nocera et al. \[NNPDF\], Nucl. Phys. B 887 \(2014\)](#)

- The **fixed-order** and **RGR** matchings show an aligned behavior at **moderate x** , where LaMET can make reliable prediction;
- Comparing with the NNPDF results, CG method gives a **consistent prediction** on the **valence part** of both the unpolarized and the helicity PDFs, which provides encouraging evidence for the **efficacy of the CG method**;
- The **small deviation of the valence part** might be caused by the **excited-state contamination** and other lattice systematics;
- The deviation of $(\Delta q - \Delta \bar{q})/2$ from the NNPDF results may be caused by systematics from **excited-state contaminations** and **renormalization of the imaginary part** of quasi PDF matrix elements, which exist in GI method as well;
- This work also serves as an examination of **universality** in LaMET.

Summary

- This is the **first lattice calculation** of the proton PDFs using the **CG method**;
- Our results for both the unpolarized and helicity PDFs show encouraging agreement with NNPDF at **moderate x of valence distribution**, while the slight deviations are likely due to the excited-state contaminations;
- The **imaginary part** corresponds to the distribution of $(q + \bar{q})/2$, which is likely more sensitive to systematics from **excited-state contaminations and renormalization**;
- We are increasing our lattice statistics at larger source-sink separations to further control the excited-state effects.

Backup

Gauge Fixing in Lattice QCD

Continuous Theory

$$F_{\text{CG}}[A, \Omega] \equiv \frac{1}{2} \sum_{\mu=1}^3 \int d^4x A_{\Omega\mu}^a(x) A_{\Omega}^{\mu a}(x)$$

$$\begin{aligned}\delta F_{\text{CG}}[A, \Omega] &= - \sum_{\mu=1}^3 \int d^4x (D_{\mu ab}^{\Omega} \theta_b) A_{\Omega}^{\mu a} \\ &= - \sum_{\mu=1}^3 \int d^4x (\partial_{\mu} \theta_a - g f^{cab} A_{\Omega\mu}^c \theta_b) A_{\Omega}^{\mu a} \\ &= \sum_{\mu=1}^3 \int d^4x \theta_a (\partial_{\mu} A_{\Omega}^{\mu a})\end{aligned}$$

Lattice Theory

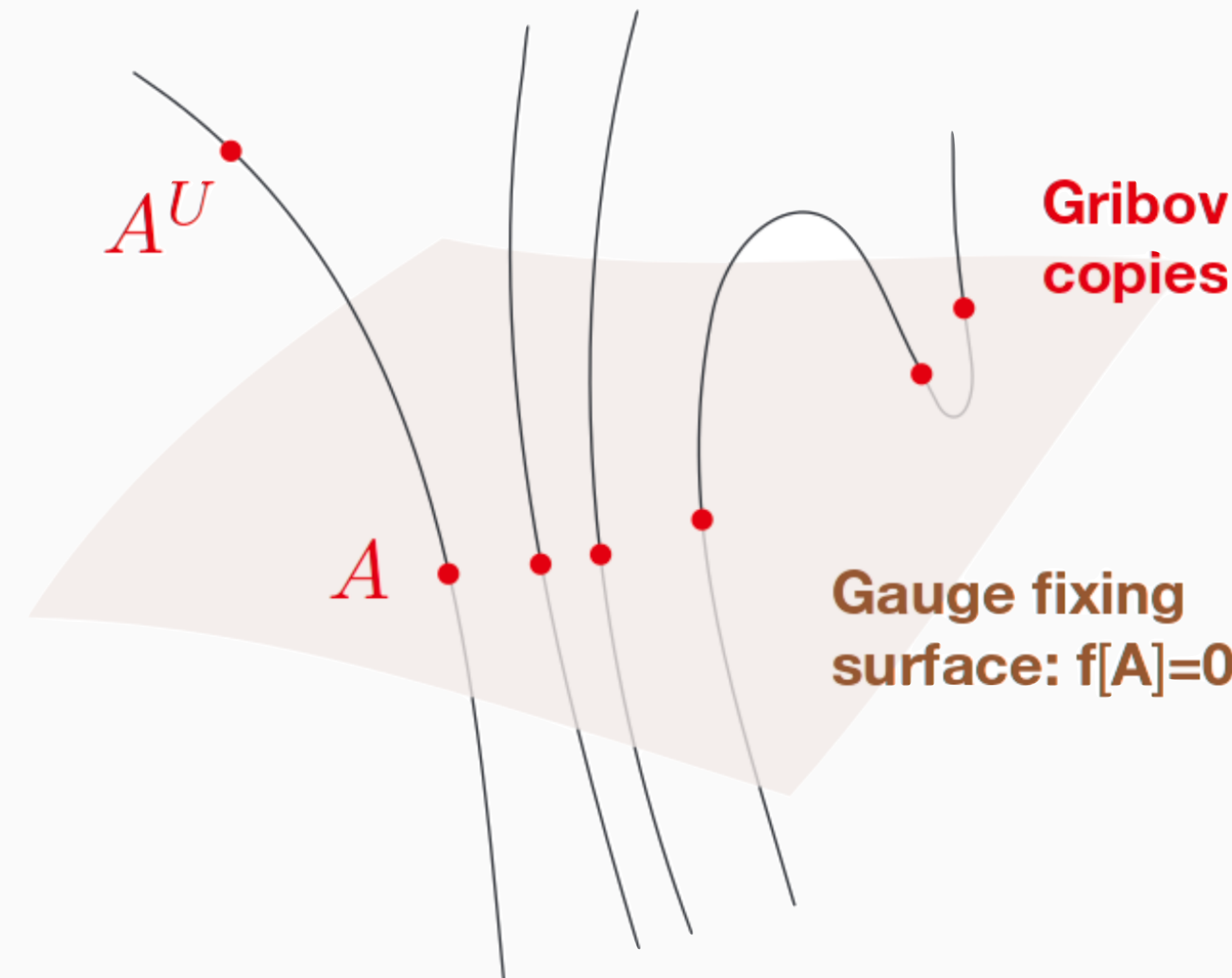
$$F_{\text{CG}}[U, \Omega] \equiv -\Re \left[\text{Tr} \sum_x \sum_{\mu=1}^3 \Omega^{\dagger}(x + \hat{\mu}) U_{\mu}(x) \Omega(x) \right]$$

Find stationary points of the functional value.

$${}^* A_{\Omega\mu}(x) \equiv \Omega^{\dagger}(x) A_{\mu}(x) \Omega(x) + \frac{i}{g} \Omega^{\dagger}(x) \partial_{\mu} \Omega(x)$$

Gribov Copies

- The gauge fixing condition may have many solutions in Lattice QCD.



Ph. D. Thesis of Diego Fiorentini

Criteria of Gauge Fixing

- Variation of the functional

$$\delta F/F < 10^{-8}$$

- Residual gradient of the functional

$$\theta^G \equiv \frac{1}{V} \sum_x \theta^G(x) \equiv \frac{1}{V} \sum_x \text{Tr} \left[\Delta^G(x) (\Delta^G)^{\dagger}(x) \right]$$
$$* \Delta^G(x) \equiv \sum_{\mu} \left(A_{\mu}^G(x) - A_{\mu}^G(x - \hat{\mu}) \right)$$

Different Gribov copies can be distinguished by the difference of functional values ΔF .

Coulomb Gauge Method

- Define a quasi correlator in CG without Wilson line, which belongs to the universality class in LaMET:

$$\tilde{f}_{\text{CG}}^0(y, P^z, \mu) = P^z \int \frac{dz}{2\pi} e^{iz(yP^z)} \frac{1}{2P^t} \langle P | \bar{\psi}_0(z) \Gamma \psi_0(0) |_{\vec{\nabla} \cdot \vec{A}=0} | P \rangle$$

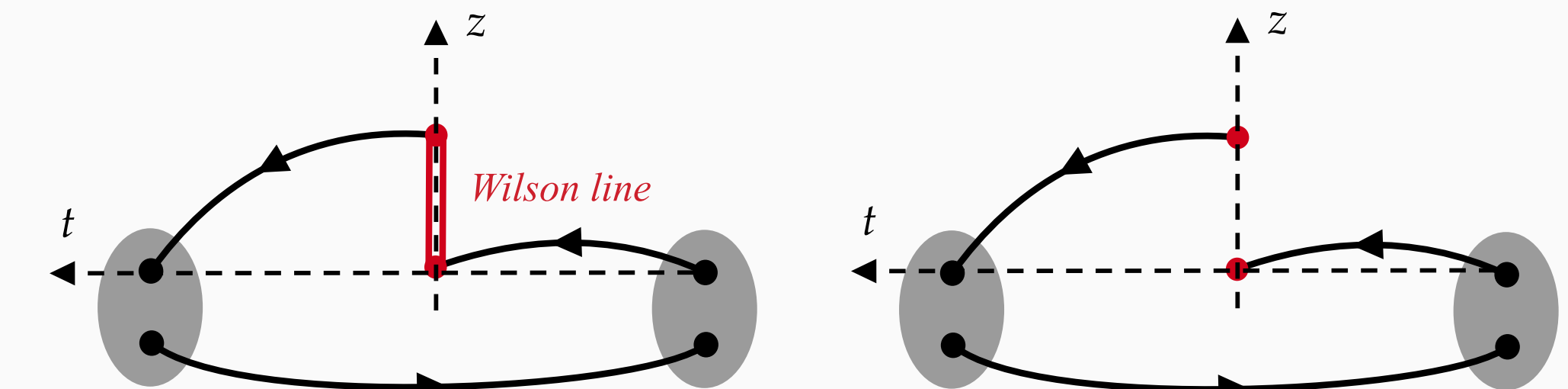
X. Ji, Y. S. Liu, Y. Liu, J. H. Zhang and Y. Zhao, RMP 93 (2021)

- Why choose CG?

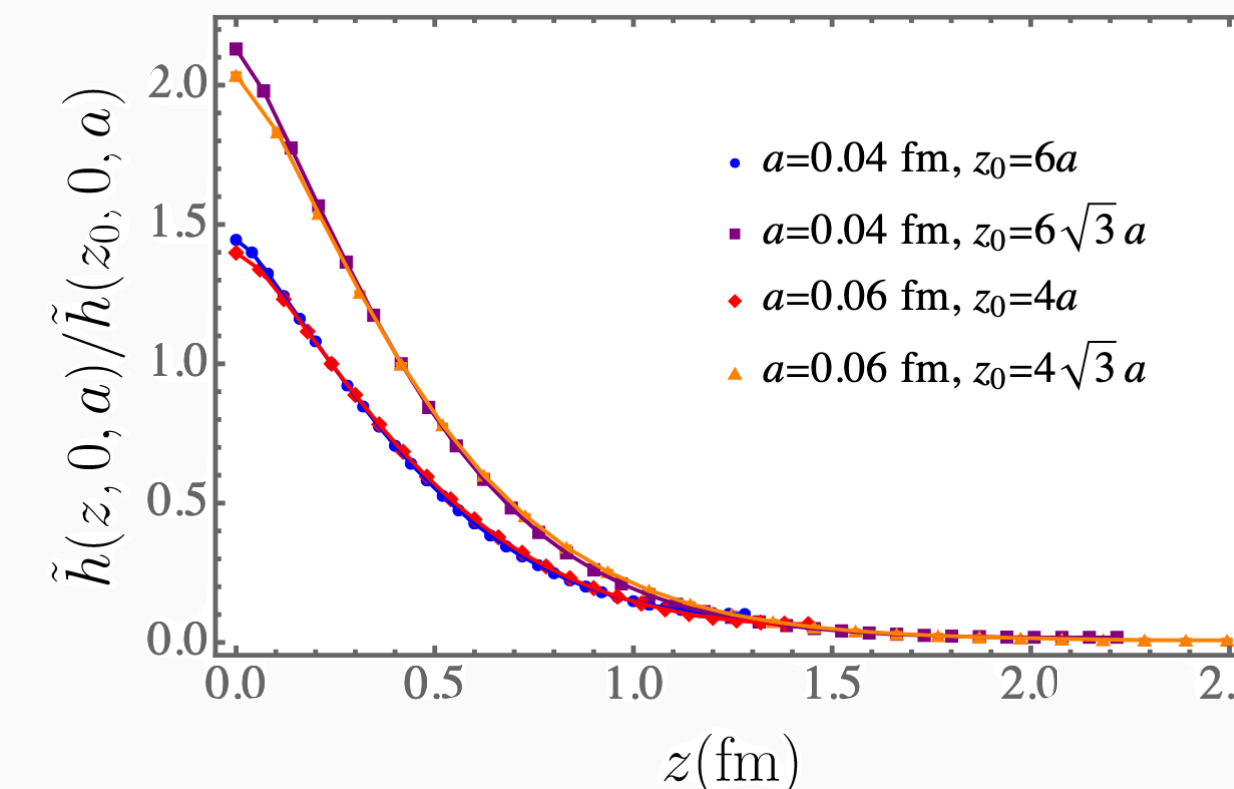
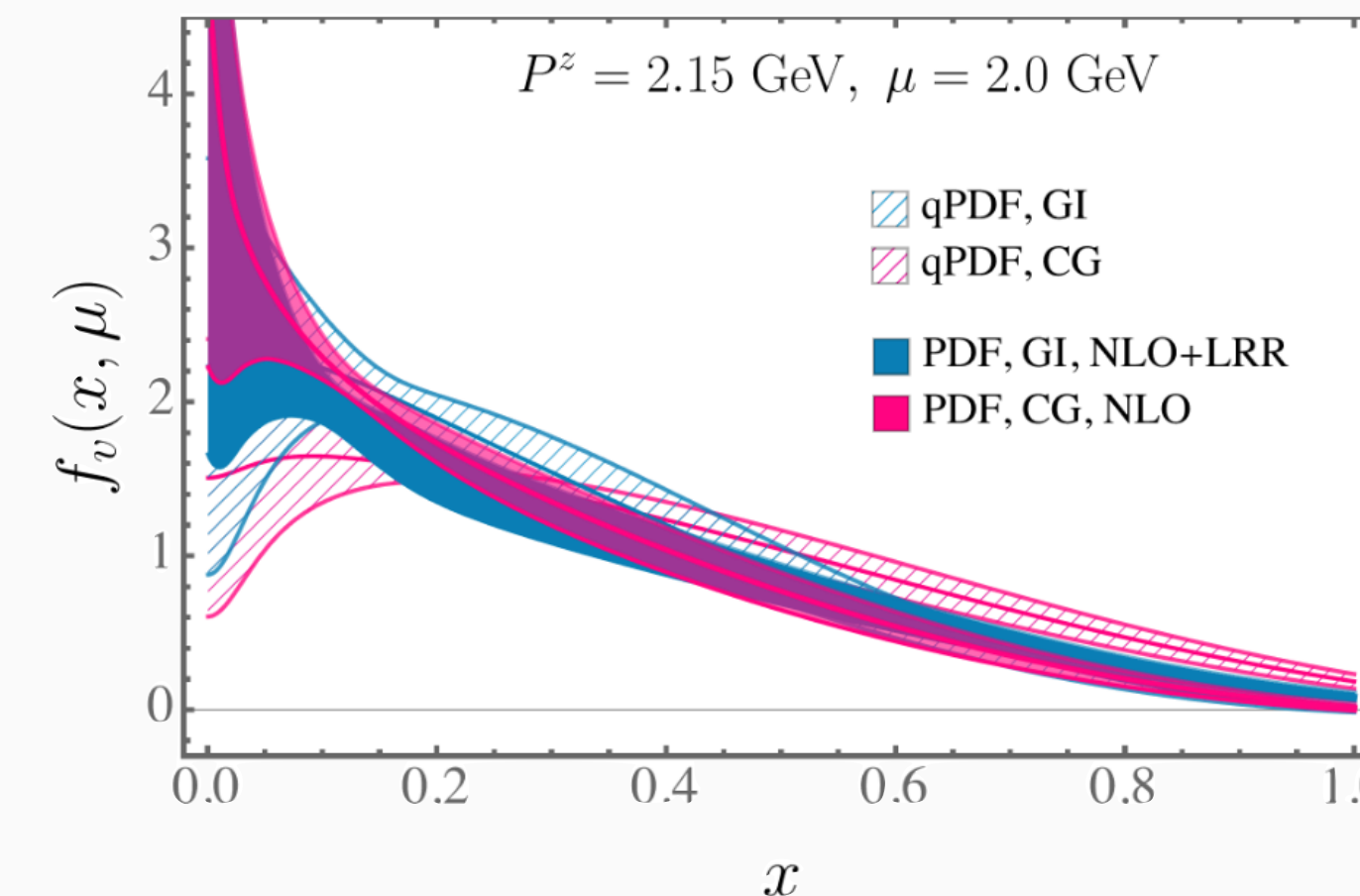
- CG becomes light-cone gauge in the infinite boost
- No linear divergence / linear renormalon
- Simplified renormalization $\bar{\psi}_0(z) \Gamma \psi_0(0) = Z_\psi [\bar{\psi}(z) \Gamma \psi(0)]$
- Larger off-axis momenta (3D rotational symmetry)

Wilson line on light-cone

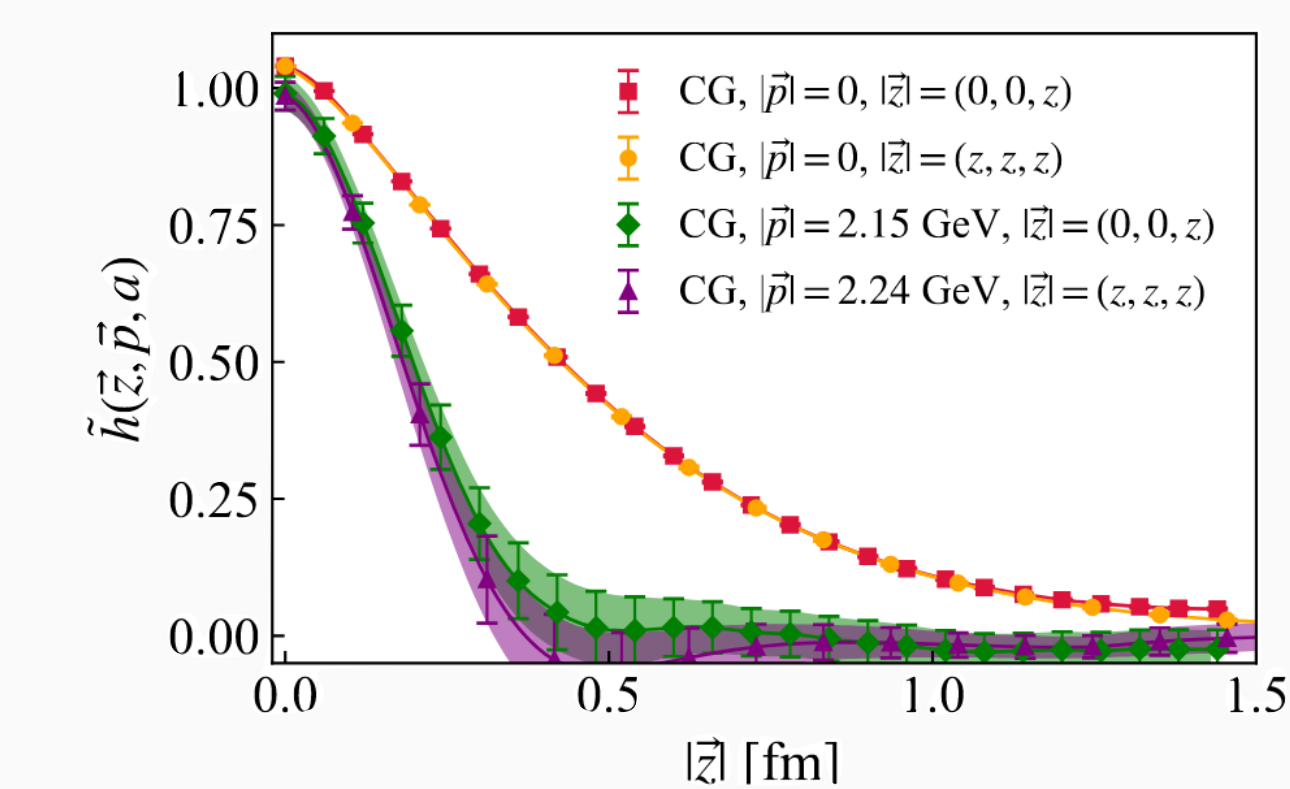
$$\psi_C(x) = e^{-ie\frac{1}{\nabla^2} \vec{\nabla} \cdot \vec{A}} \psi_0(x) \xrightarrow{P^z \rightarrow \infty} e^{-ie\frac{1}{(\nabla^+)^2} \nabla^+ A^+} \psi_0(x) = e^{-ie\frac{1}{\nabla^+ \pm 0} A^+} \psi_0(x) = e^{-ie \int_{\pm \infty}^x dy^- A^+(y^-, x_\perp)} \psi_0(x)$$



Pion valence PDF in CG v.s. GI



Gauge Invariant (GI)



Coulomb Gauge (CG)